SINAP 中国科学院上海应用物理研究所
Shanghai Institute of Applied Physics, Chinese Academy of Sciences

相变与机器学习

原子核结构与中高能重离子碰撞交叉学科理论讲习班

王睿

中国科学院上海应用物理研究所 (SINAP)

合作导师: 马余刚 (SINAP, FDU)

- 铁磁相变与Ising模型
- 核物质的液气相变
- QCD相图

Ising model and Ferromagnetic phase transition

Ising model(伊辛模型) $$H = -J \sum_{ij} \sigma_i^z \sigma_j^z$$

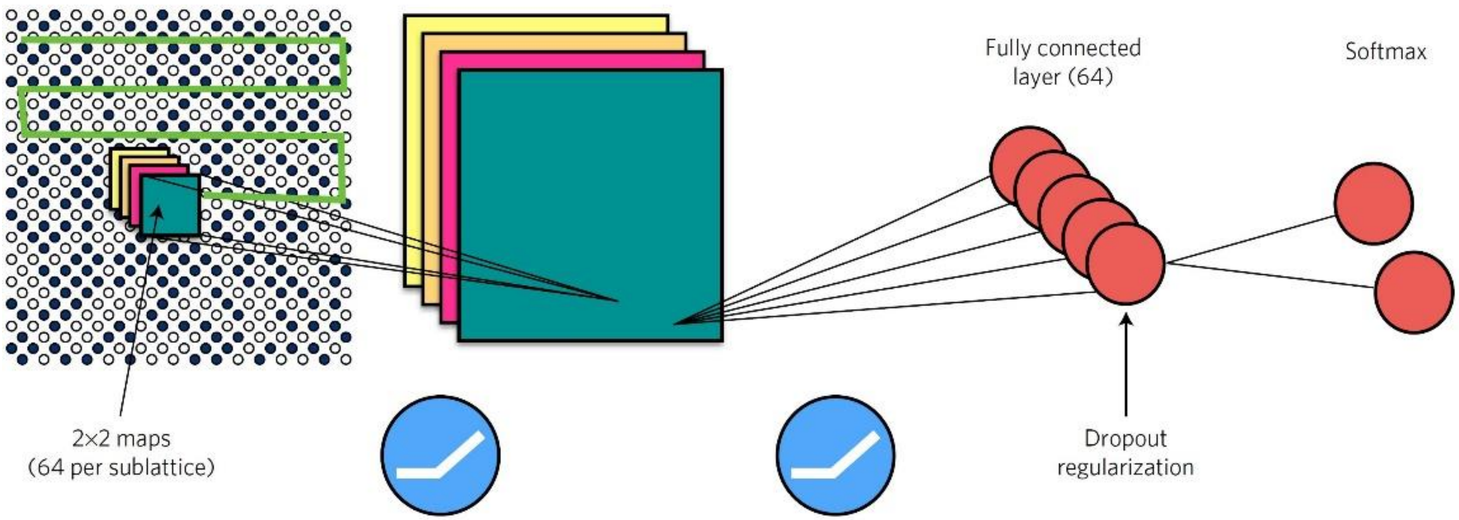

Configurations in Ising model, spin up or down, generated by standard Monte Carlo techniques for different temperature.

Since the critical temperature in Ising model can be calculated analytically

the images are divided into two categories labeled as low-temperature ferromagnetic and high-temperature paramagnetic.

J. Carrasquilla & R. G. Melko, Nature Physics **13**, 431-434 (2017)

Ising model and Ferromagnetic phase transition

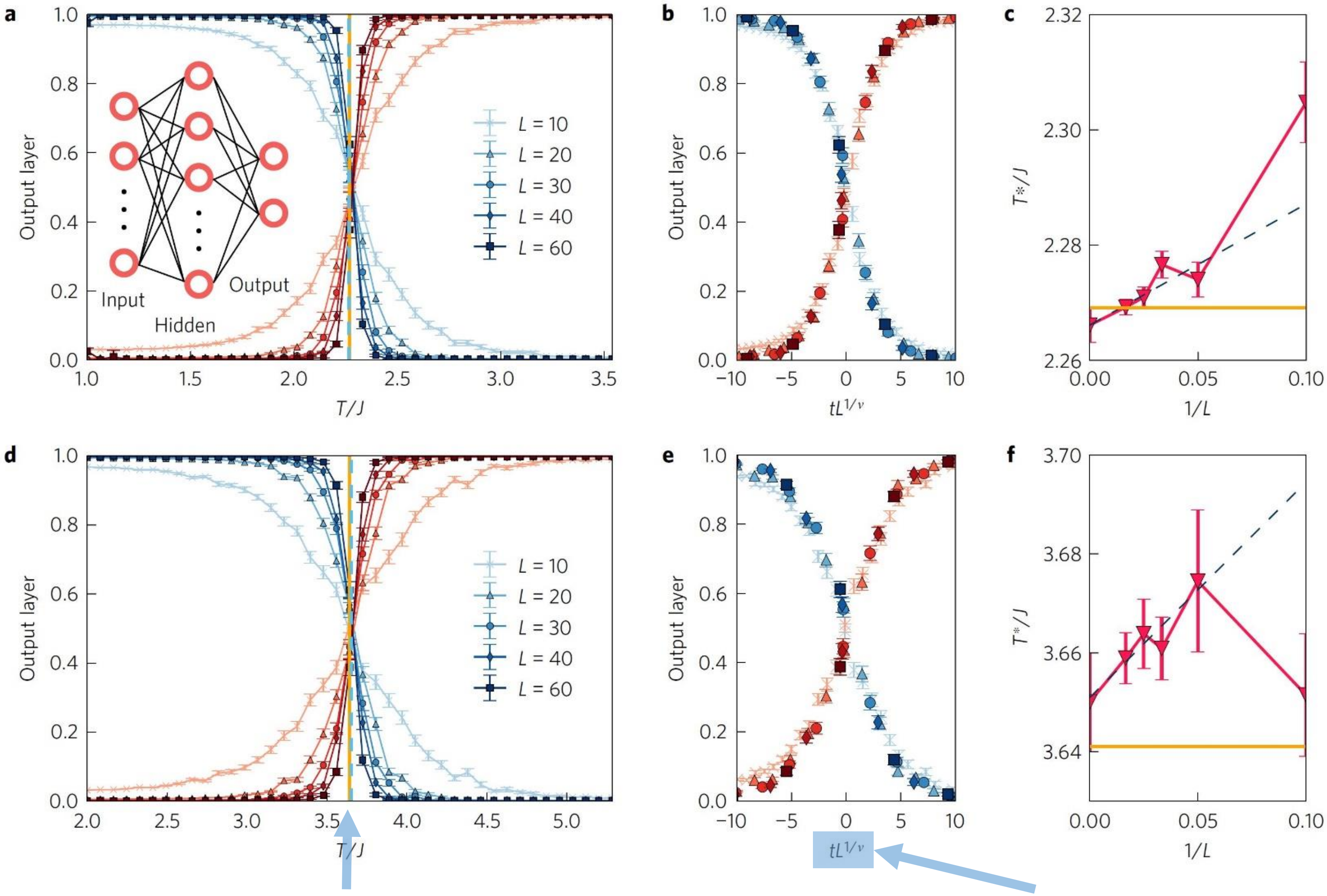

Critical point T_c Critical exponent $\nu = 1.0 \pm 0.2$

J. Carrasquilla & R. G. Melko, Nature Physics **13**, 431-434 (2017)

Basic concepts for phase transitions

Critical exponents (临界指数)

$$m(T, h=0) \propto \begin{cases} 0 & \text{for } T > T_c \\ |t|^\beta & \text{for } T < T_c \end{cases}$$

Describe the non-analyticity of various thermodynamic functions

$$t \equiv (T - T_c)/T_c$$

- Order parameters (序参量)

  A thermodynamic function that is different in each phase, and hence can be used to distinguish between them
  Magnetization m for ferromagnetic phase transition
  Density difference $\rho_l - \rho_g$ for liquid-gas phase transition

- Response functions (响应函数)

  The change of a quantity with respect to external perturbations
  Susceptibility χ, heat capacity C

- Long-range correlations (长程关联)

  Correlated fluctuations over large distances
  Correlation length ξ

Landau-Ginzburg Hamiltonian

$$\beta\mathcal{H} = \beta F_0 + \int d^d\mathbf{x}\Big[\frac{t}{2}m^2(\mathbf{x}) + um^4(\mathbf{x}) + \frac{K}{2}(\nabla m)^2 + \cdots - \vec{h}\cdot\vec{m}(\mathbf{x})\Big]$$

$$a \text{ (microscopic scale)} \ll \mathbf{x} \ll L \text{ (macroscopic scale)}$$

Saddle point approximation

$$\begin{aligned} Z &= \int \mathcal{D}\vec{m}(\mathbf{x})\exp\{-\beta\mathcal{H}[\vec{m}(\mathbf{x})]\} \\ &\approx Z_{sp} = e^{-\beta F_0}\int d\vec{m}\,\exp\Big[-V\Big(\frac{t}{2}m^2 + um^4 + \cdots - \vec{h}\cdot\vec{m}\Big)\Big] \end{aligned}$$

In the limit of $V \to \infty$ the integral is governed by the saddle point $\vec{m}$

$$\beta F_{\rm sp} = -\ln Z_{\rm sp} \approx \beta F_0 + V\min\Big\{\frac{t}{2}m^2 + um^4 + \cdots - \vec{h}\cdot\vec{m}\Big\}_{\vec{m}}$$

Landau-Ginzburg Hamiltonian

$$\min\left\{\frac{t}{2}m^2 + um^4 + \cdots - \vec{h}\cdot\vec{m}\right\}_{\vec{m}}$$

Note the minimization operation
is not an analytic procedure

For positive t

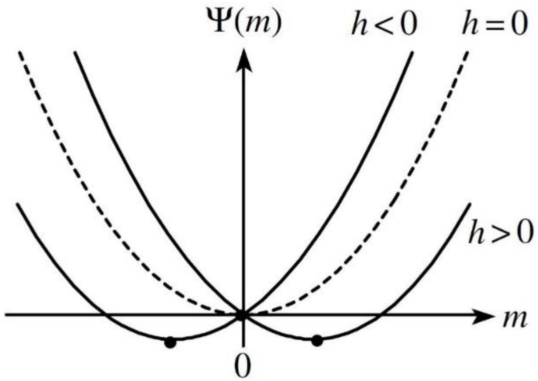

For negative t

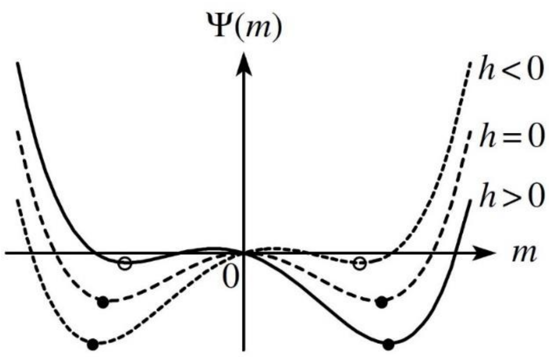

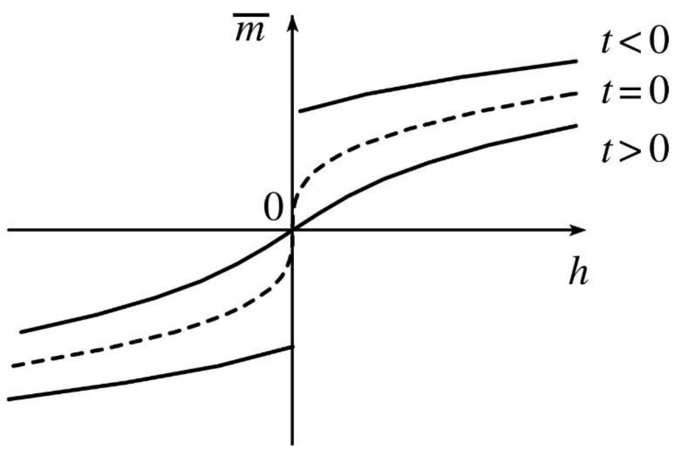

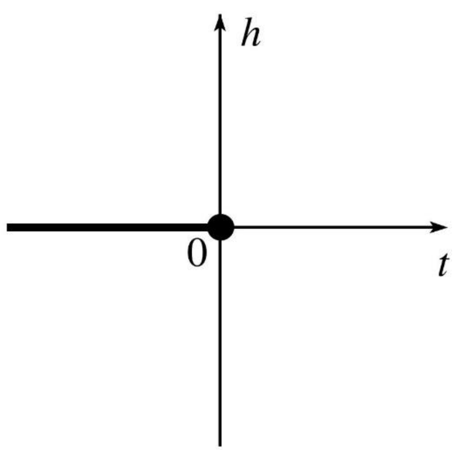

Landau-Ginzburg Hamiltonian

$$\min\left\{\frac{t}{2}m^2 + um^4 + \cdots - \vec{h}\cdot\vec{m}\right\}_{\vec{m}}$$

We then have

$$t\overline{m} + 4u\overline{m}^3 + \cdots - h = 0$$

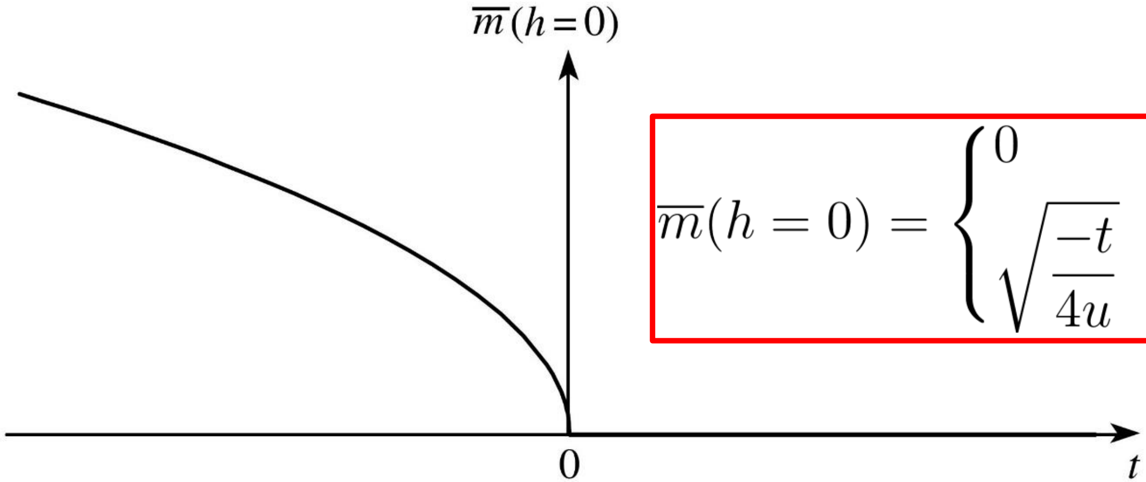

$$\overline{m}(h=0) = \begin{cases} 0 & \text{for } t > 0 \\ \sqrt{\dfrac{-t}{4u}} & \text{for } t < 0 \end{cases}$$

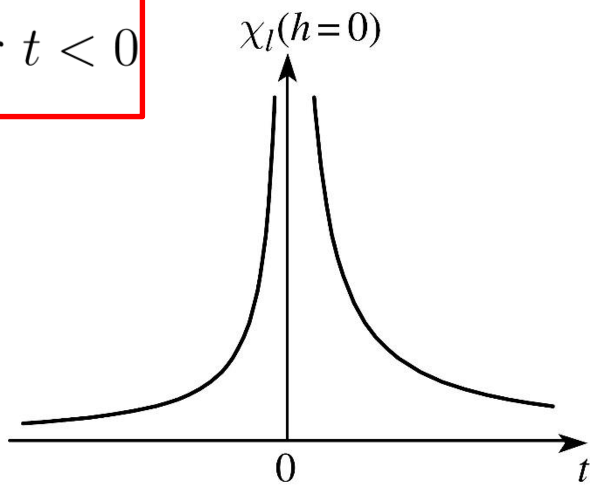

$$\overline{m}(t=0) = \left(\frac{h}{4u}\right)^{1/3}$$

$$\chi_l^{-1} = \frac{\partial h}{\partial \overline{m}}\bigg|_{h=0} = t + 12u\overline{m}^2\bigg|_{h=0} = \begin{cases} t & \text{for } t > 0, \text{ and } h = 0 \\ -2t & \text{for } t < 0, \text{ and } h = 0 \end{cases}$$

The scaling hypothesis

Liquid-gas co-existence line of eight different matter

Critical exponent
for order parameter

$$(\rho_l - \rho_g) \propto \begin{cases} 0 & \text{for } t > T_c \\ |t|^\beta & \text{for } T < T_c \end{cases}$$

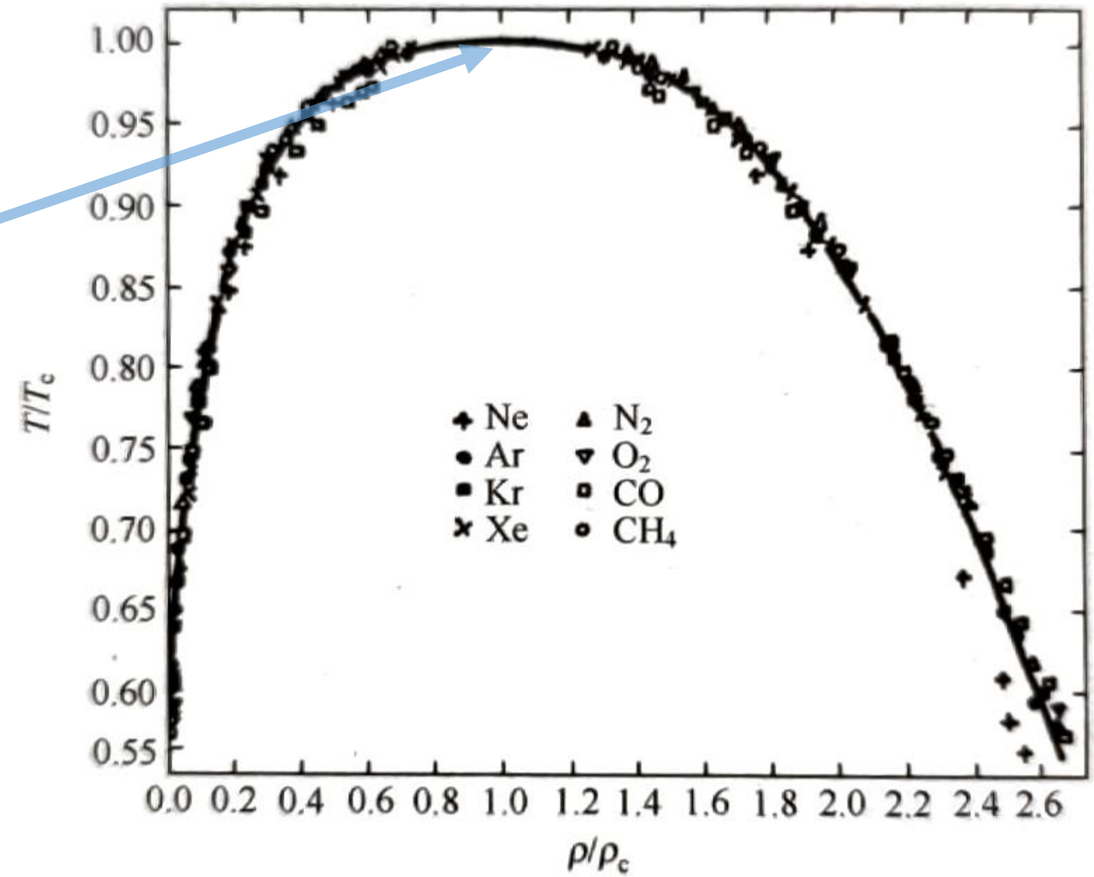

The renormalization group

The divergence of the correlation length ξ at the critical point

Starting with the most general Hamiltonian allowed by symmetries

$$\beta\mathcal{H} = \int d^d\mathbf{x}\left[\frac{t}{2}m^2(\mathbf{x}) + um^4(\mathbf{x}) + \frac{K}{2}(\nabla m)^2 + \frac{L}{2}(\nabla^2 m)^2 + \cdots - \vec{h}\cdot\vec{m}(\mathbf{x})\right]$$

A particular system $\leftrightarrow$ a point in the parameter space $S \equiv (t, u, K, L, h, \cdots)$

1. Coarse grain $\qquad \vec{m}(\mathbf{x}) = \frac{1}{b^d}\int_{\text{Cell centered at }\mathbf{x}} d^d\mathbf{x}'\vec{m}(\mathbf{x}')$

2. Rescale $\qquad \mathbf{x}_{\text{new}} = \frac{1}{b}\mathbf{x}_{\text{old}}$

3. Renormalize $\qquad \vec{m}_{\text{new}}(\mathbf{x}_{\text{new}}) = \frac{1}{\zeta b^d}\int_{\text{Cell centered at }b\mathbf{x}_{\text{new}}} d^d\mathbf{x}'\vec{m}(\mathbf{x}')$

The renormalization group

After one RG operation, the Hamiltonian changes

$$(t, u, K, L, h, \cdots) \to (t', u', K', L', h', \cdots)$$

$$S' = \hat{\mathcal{R}}_b S$$

RG flow

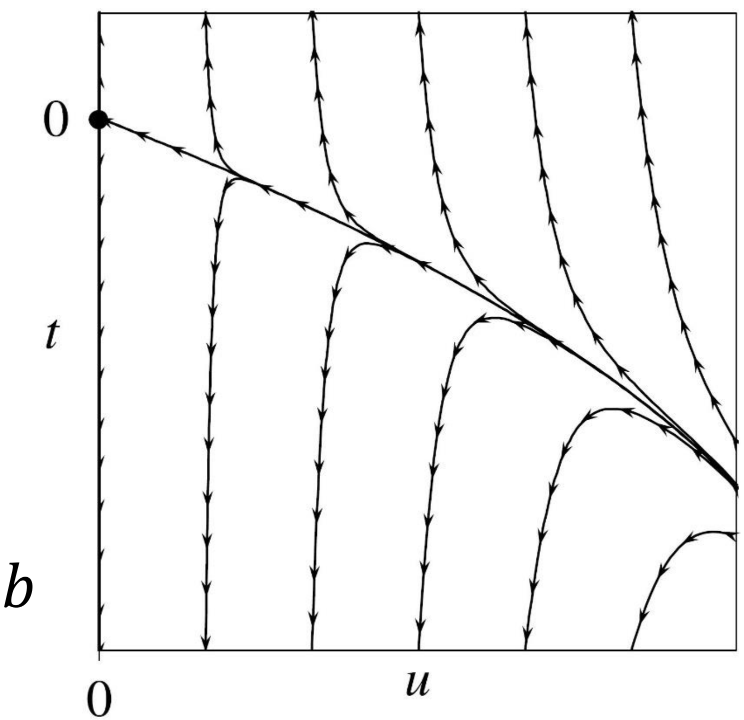

parameter space
$S \equiv (t, u, K, L, h, \cdots)$

Hamiltonians that describe statistically self-similar configurations must thus correspond to fixed points $S^* = \hat{\mathcal{R}}_b S^*$

The correlation length ξ is reduced by b under the RG operation $\xi(\hat{\mathcal{R}}_b S) = \xi(S)/b$

The critical point corresponds to the fixed point where $\xi = \infty$

The renormalization group

The renormalized parameter must be analytic functions of the original ones

$$\begin{cases} t_b(t,h) = A(b)t + \cdots \\ h_b(t,h) = D(b)h + \cdots \end{cases}$$

Consider the group property

$$t_{b_1 b_2} = A(b_1 b_2)t = A(b_1)A(b_2)t$$

$A(b)$ and $D(b)$ must be power functions

$$\begin{cases} t_b(t,h) = b^{y_t} t + \cdots \\ h_b(t,h) = b^{y_h} h + \cdots \end{cases}$$

t must be a relevant parameter

The correlation length

$$\xi(t,h) = b\xi(b^{y_t}t, b^{y_h}h) = \boxed{t^{-1/y_t}}\xi(1, h/t^{y_h/y_t})$$

Critical exponent for ξ

At fixed points S^*

$y > 0$ relevant parameter

$y < 0$ irrelevant parameter

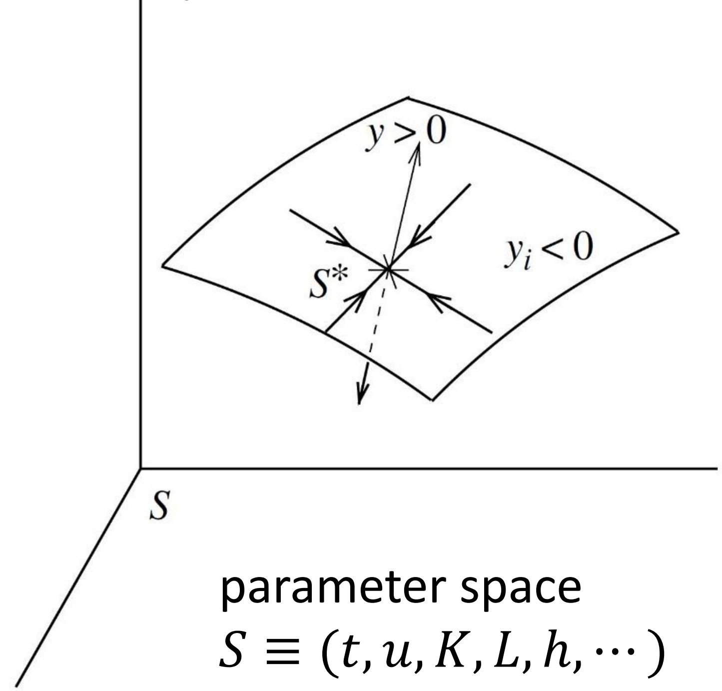

parameter space

$S \equiv (t, u, K, L, h, \cdots)$

Ising model and Ferromagnetic phase transition

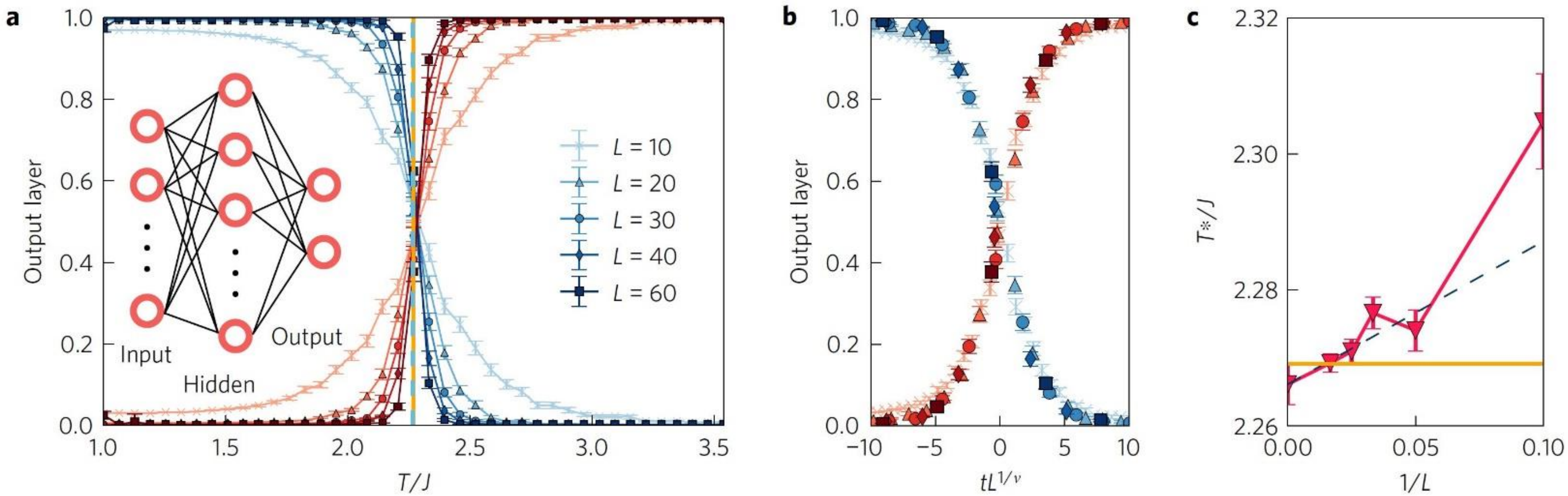

Changes in L can be regards as RG operations

$$b = L/L' \quad \text{and} \quad \xi' = \xi/b$$

$$\xi/L \propto t^{-\nu}/L \text{ is independent of } L$$

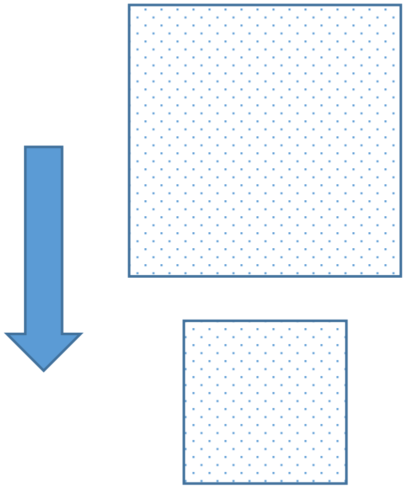

J. Carrasquilla & R. G. Melko, Nature Physics **13**, 431-434 (2017)

Ferromagnetic phase transition

Principal component analysis (主成分分析)

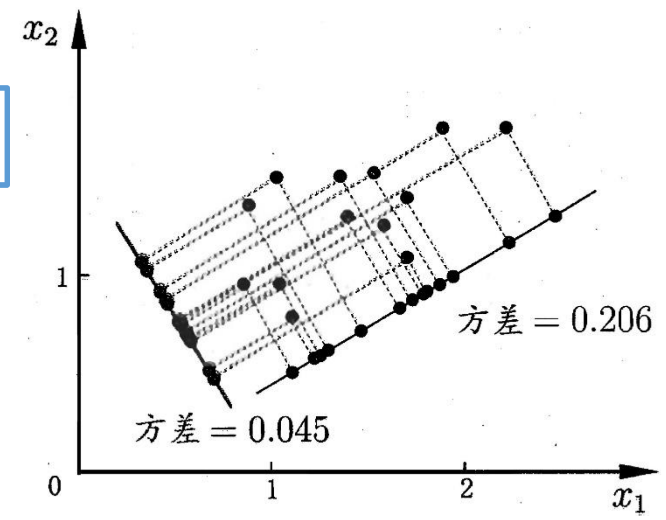

$$S = \frac{1}{N^2} \sum_{i,j} [\cos(\theta_i - \theta_j) + \cos(\phi_i - \phi_j)]$$

Related to the first 4 principal components

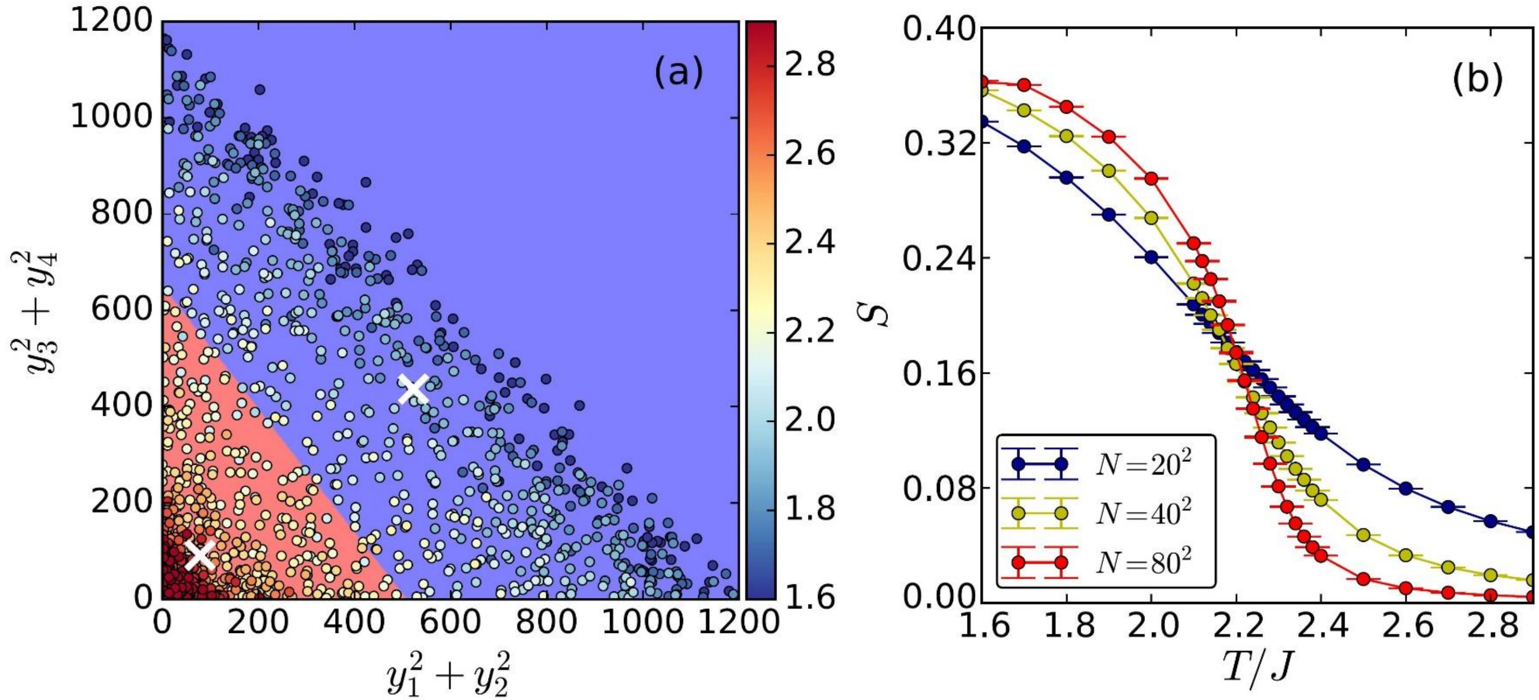

L. Wang, Physical review B **94**, 195105 (2016)

Ferromagnetic phase transition

Auto-encoder network

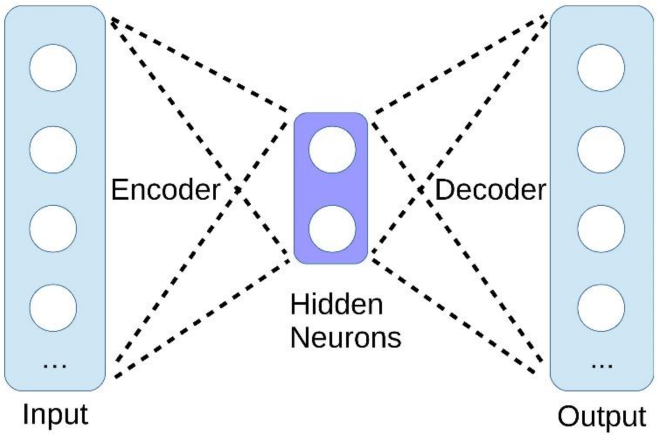

Spin configurations in Ising model before and after encoding

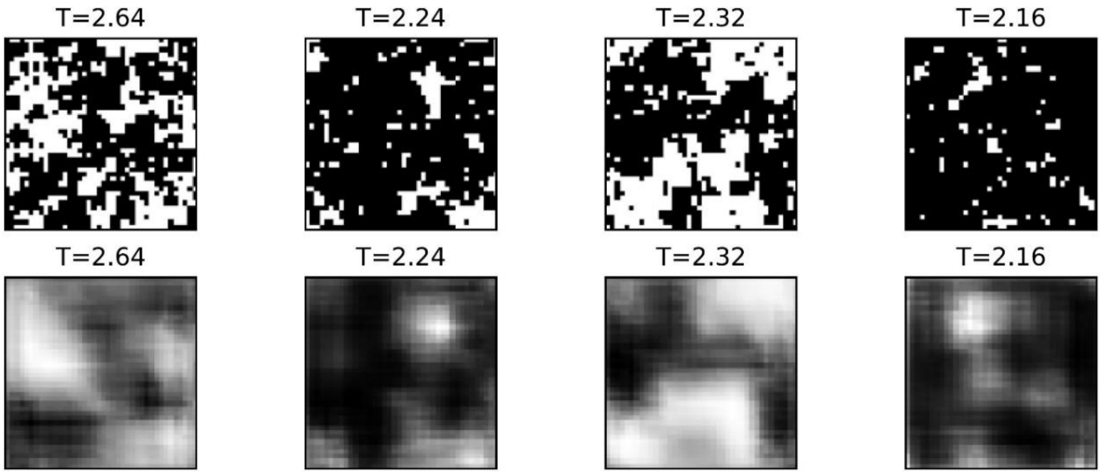

Hidden variable

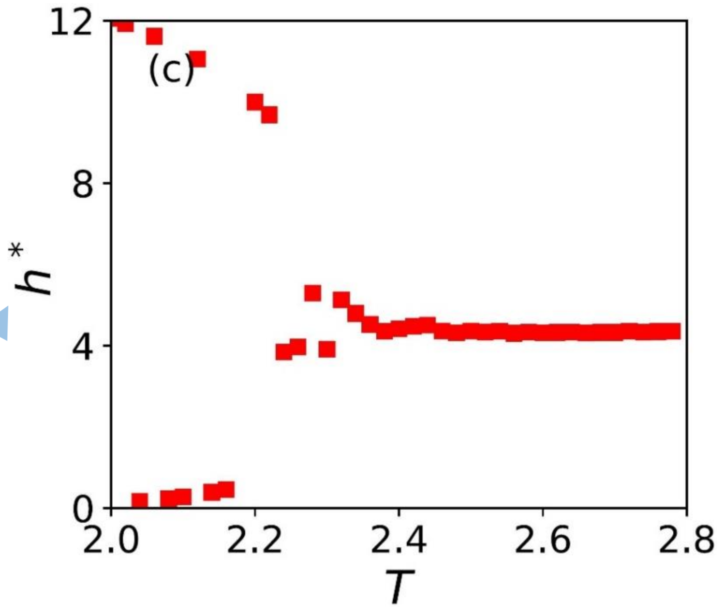

Can be regarded as an order parameter

W. Hu, R. R. P. Singh & R. T. Scalettar, Physical review E **95**, 062122 (2017)

Ferromagnetic phase transition

Confusion scheme

For Ising model

Dividing the samples into two categroies by a proposed critial $T_c{}'$

Different $T_c{}'$ leads to different total testing accuracy of the network

The real critical point T_c can be deduced from the performance curve

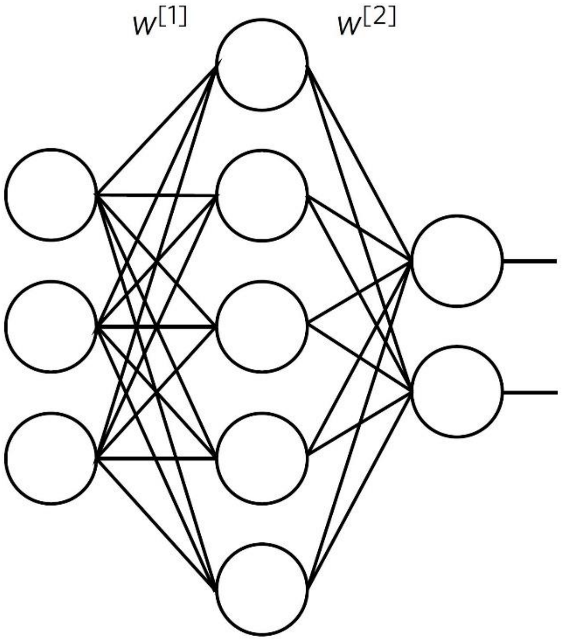

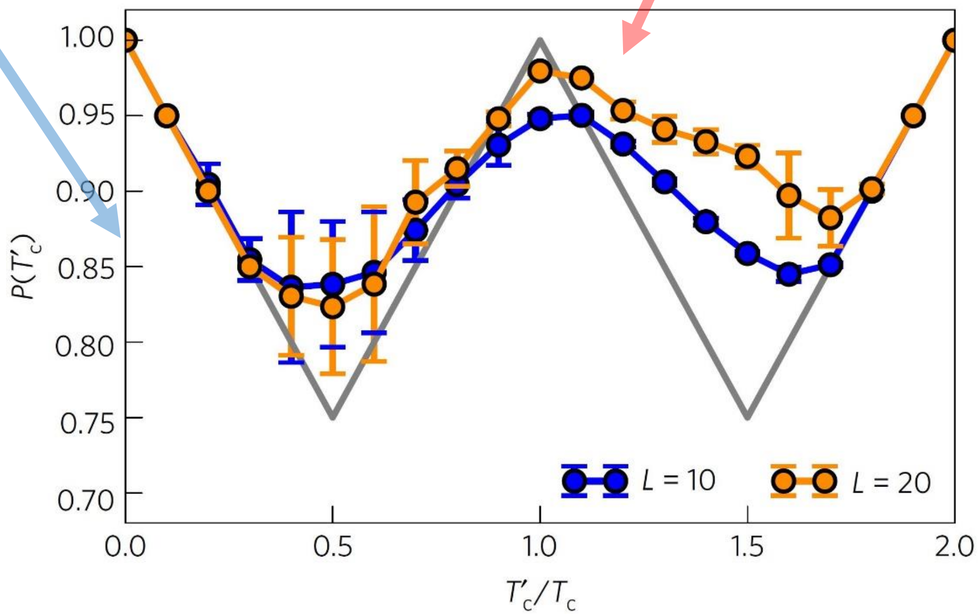

E. P. L. van Nieuwenburg, Y.-H. Liu & S. D. Huber, Nature physics **13**, 435–439 (2017)

Nuclear liquid-gas phase transition

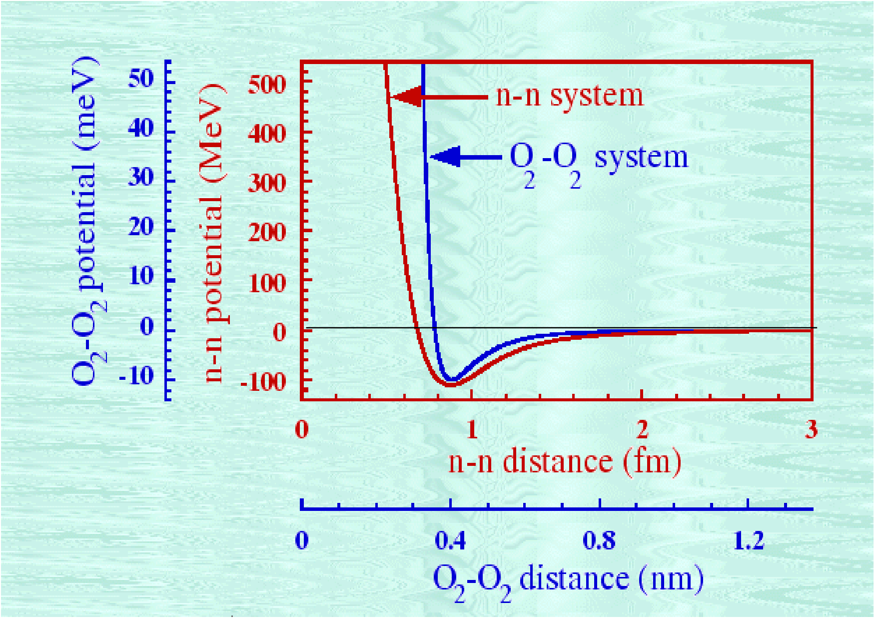

The interaction between nucleons exhibit Van der Waals features, thus the nuclei can experience liquid-gas phase transition

The nucleus is an uncontrollable system

Phase transition in condensed matter
1. Number of molecule ~ 10^{23} (Avogadro number)
2. Easy to heat up by a static way
3. Easy to measure temperature

Phase transition in nuclear matter
1. Number is up to several hundred. (a large fluctuation)
2. Nuclear reaction is used to heat up (dynamical process)
3. not easy to measure the temperature.

Nuclear liquid-gas phase transition

A simple Skyrme type nucleon-nucleon effective interaction

$$v_{12} = t_0(1 + x_0\hat{P}_\sigma)\delta(\vec{r}_1 - \vec{r}_2) + \frac{1}{6}t_3(1 + x_3\hat{P}_\sigma)\rho^\alpha(\frac{\vec{r}_1 + \vec{r}_2}{2})\delta(\vec{r}_1 - \vec{r}_2)$$

$$\int \varepsilon(\vec{r})d^3r = \sum_i \langle i|\frac{p^2}{2m}|i\rangle + \frac{1}{2}\sum_{i,j}\langle ij|v_{12}|ij\rangle$$

$$\sim \text{a functional of } f(\vec{r},\vec{p})$$

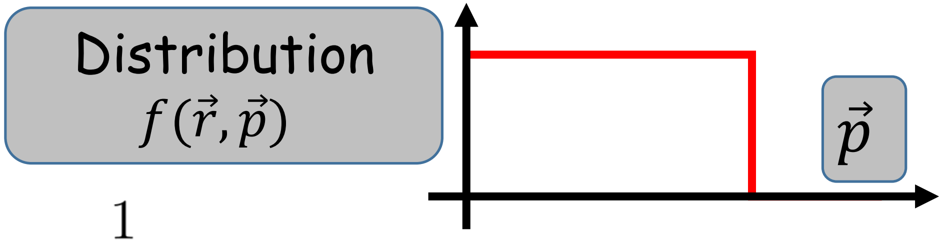

Fermi distribution $\quad f(\vec{r},\vec{p}) \propto \dfrac{1}{1 + \exp\{\frac{\varepsilon[\vec{p},f(\vec{r},\vec{p})]-\mu}{k_B T}\}}$

Energy per nucleon or equation-of-state $\quad E = E(\rho, \delta, T)$

Entropy $\quad S \propto \int_0^\infty dpp^2[f\ln f + (1-f)\ln(1-f)]$

Pressure can be obtained from thermodynamic relation

Nuclear liquid-gas phase transition

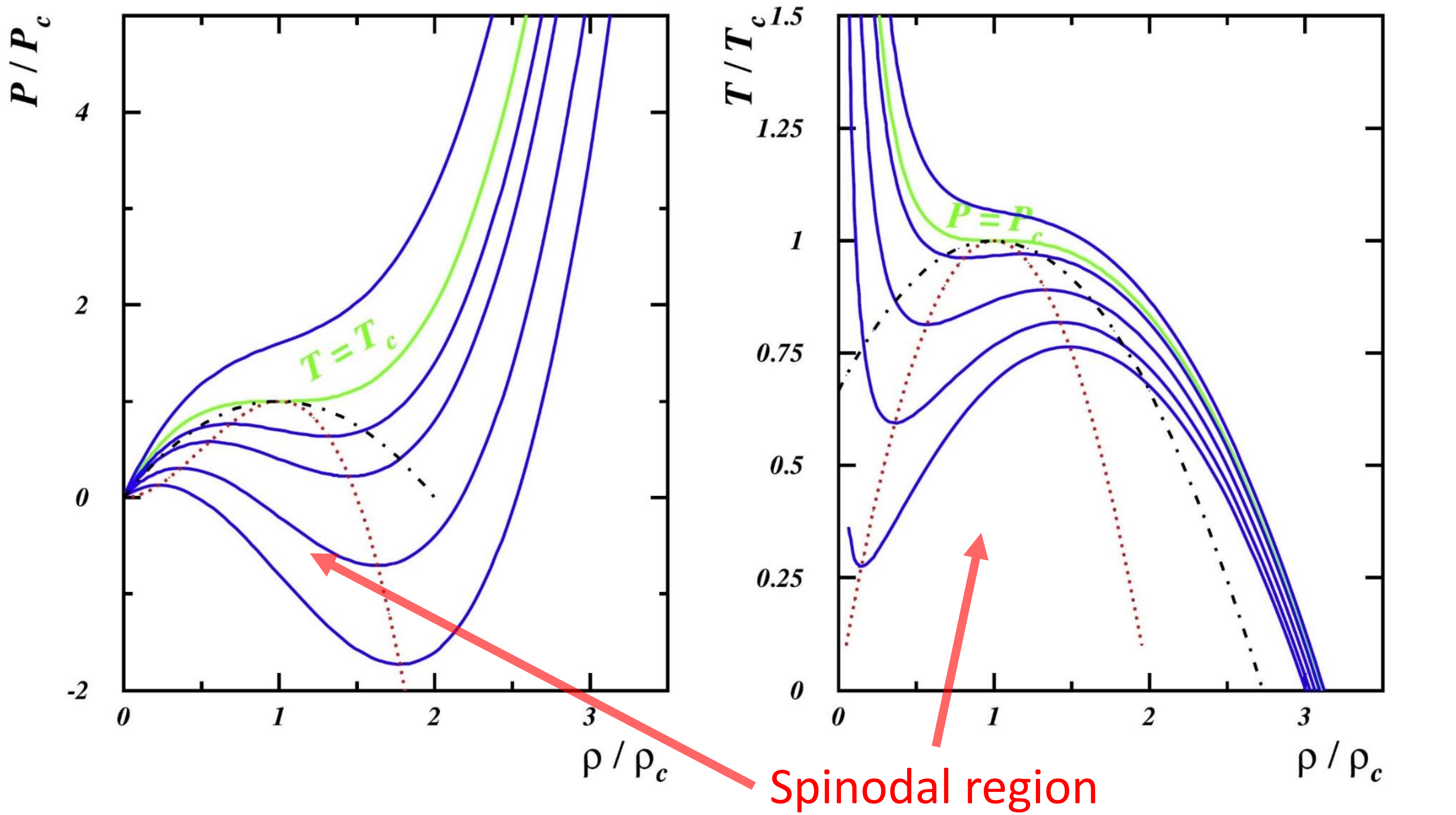

B. Borderie & J.D. Frankland, Progress in Particle and Nuclear Physics 105 (2019) 82–138

Nuclear liquid-gas phase transition

Consider another degree of freedom - Isospin asymmetry $\delta = \frac{\rho_n - \rho_p}{\rho_n + \rho_p}$

Maxwell construction

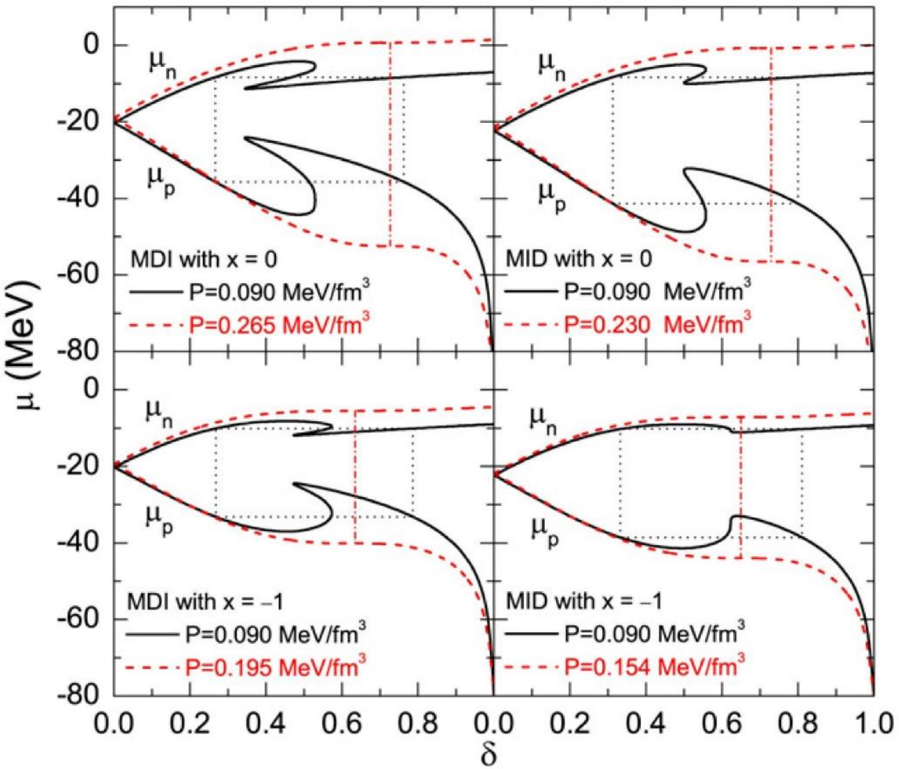

Co-existence line

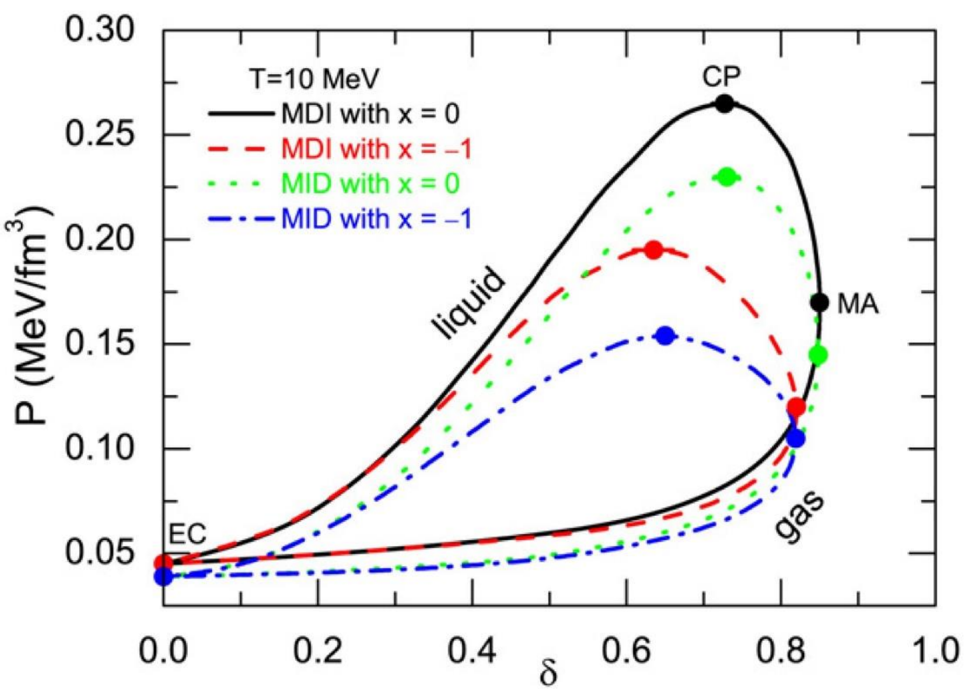

J. Xu et al., Physics Letters B 650 (2007) 348–353

Nuclear liquid-gas phase transition

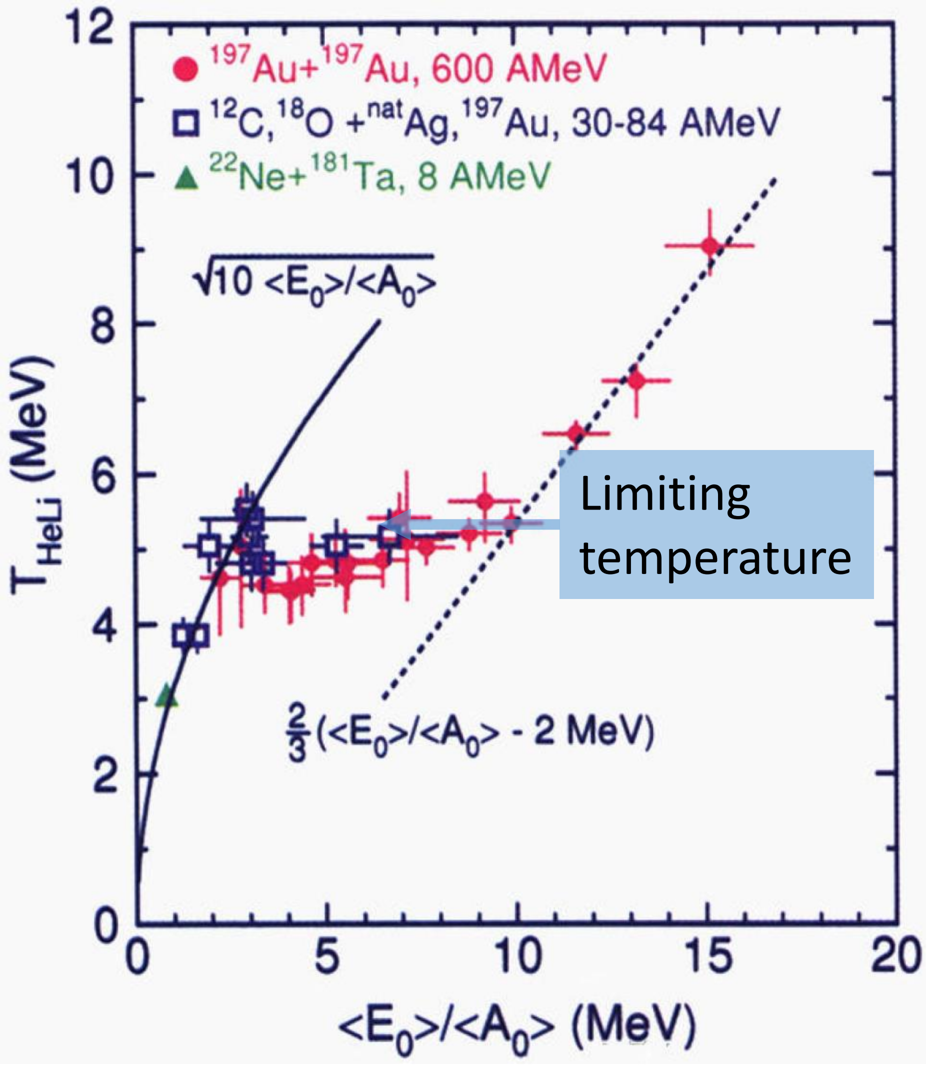

J. Pochodzalla, *et. al.*, PRL75, 1040-1043, (1995)

Heavy-ion collisions

Caloric curves

Note its difference with that in condensed matter physics

Unknown external condition

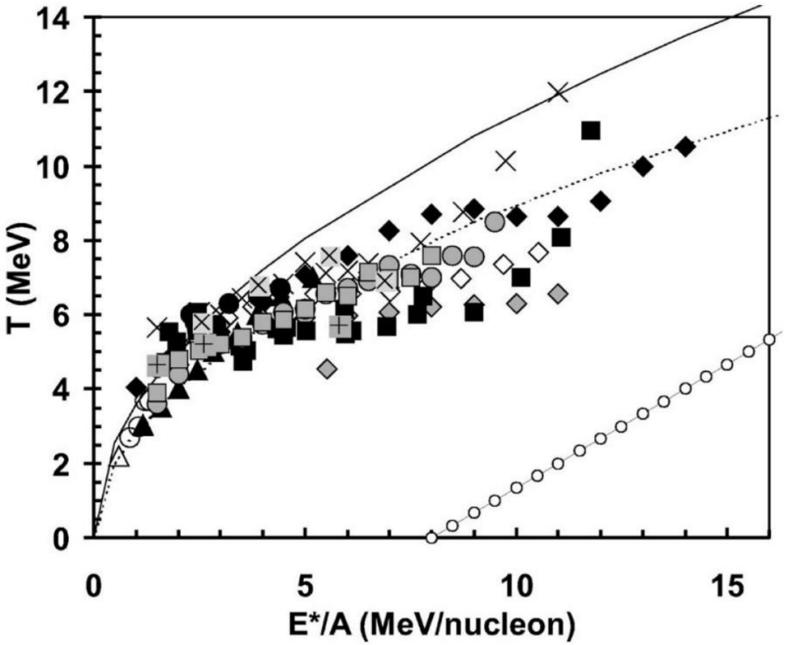

J. B. Natowitz, *et. al.*, PRC65, 034618, (2002)

Nuclear liquid-gas phase transition

The nuclear liquid-gas phase transition is realized through tracing the effect of spinodal instability, i.e., nuclear mult-fragmentation

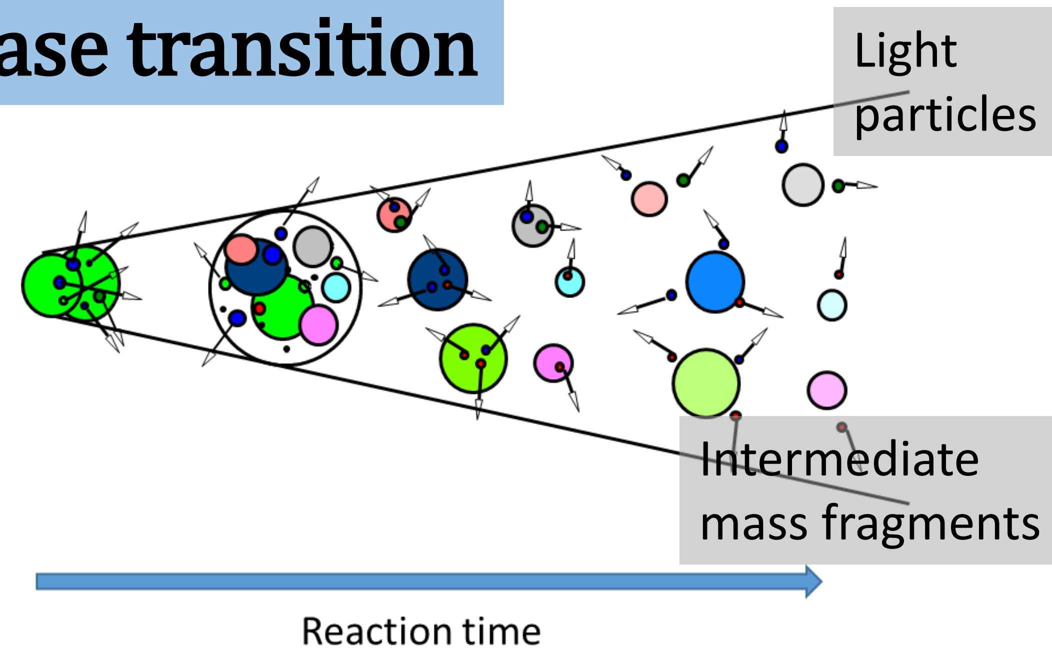

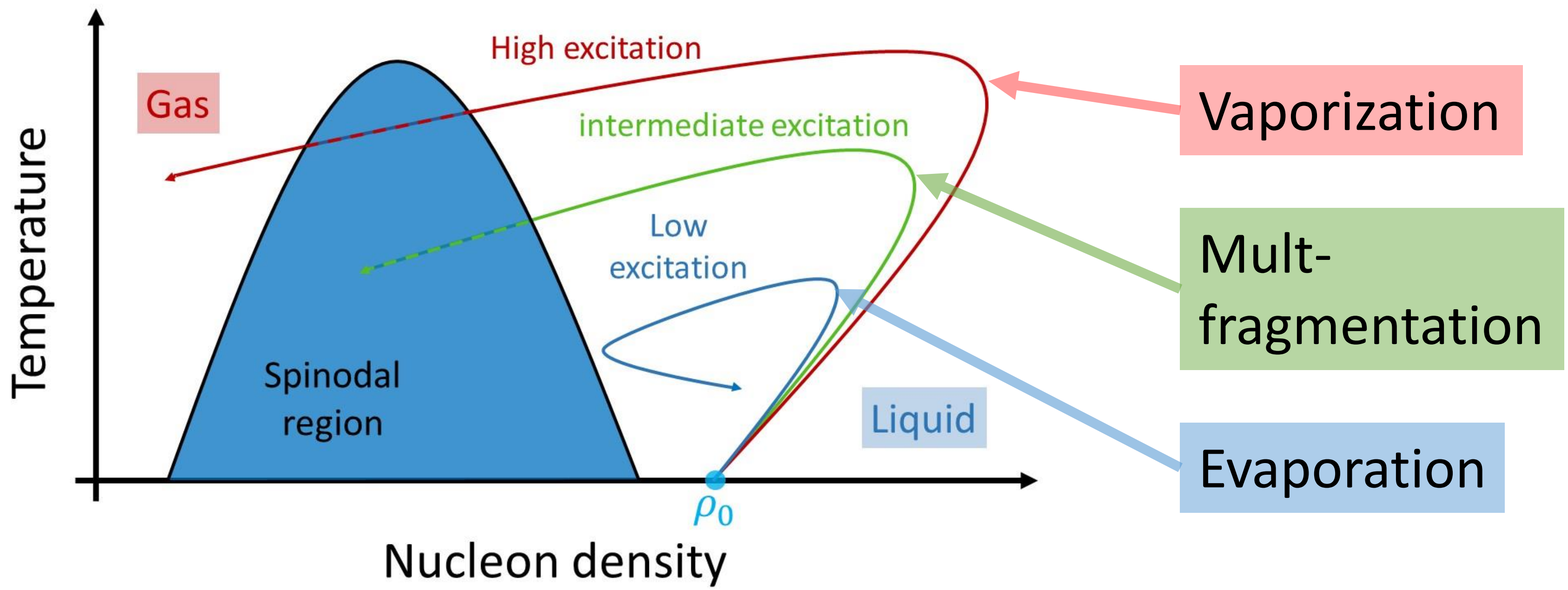

The experiment

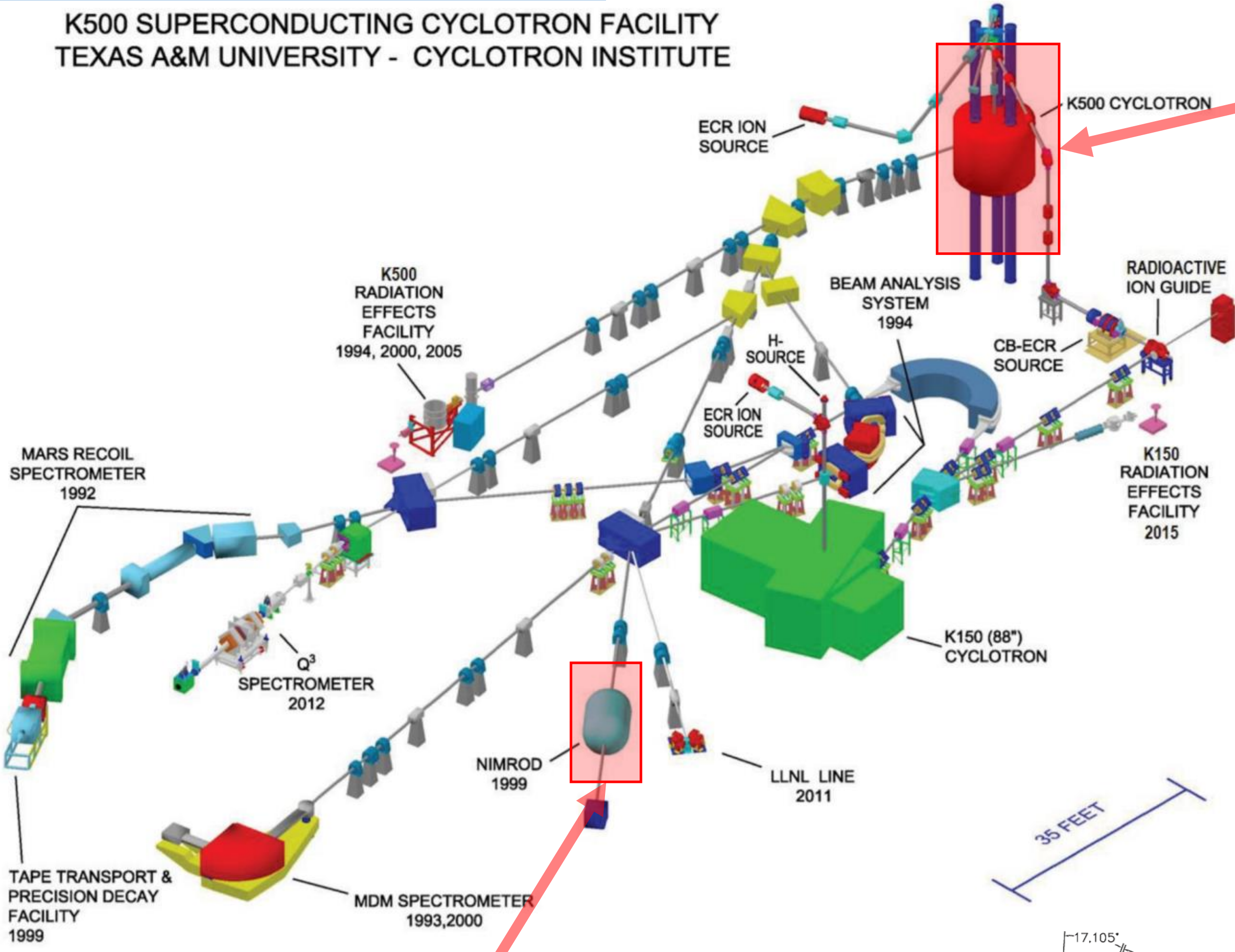

K500 super-conducting cyclotron

$$^{40}\mathrm{Ar} \rightarrow {}^{27}\mathrm{Al}$$
$$^{40}\mathrm{Ar} \rightarrow {}^{48}\mathrm{Ti}$$

At 47 MeV/A

Charge (mass) and momentum of charged particles

neutron multiplicity

4π detector NIMROD

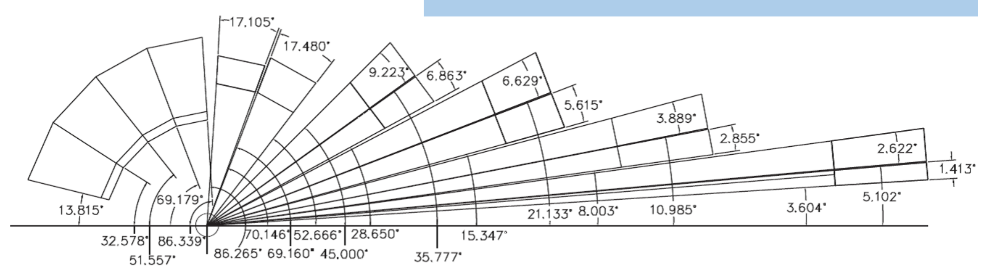

Quasi-projectile (QP) fragments

We use a three source fit to reconstruct each event and separate the QP fragments

Z^{QP} is usually less than the charge of the projectile

Nucleon-nucleon source

Quasi-target source

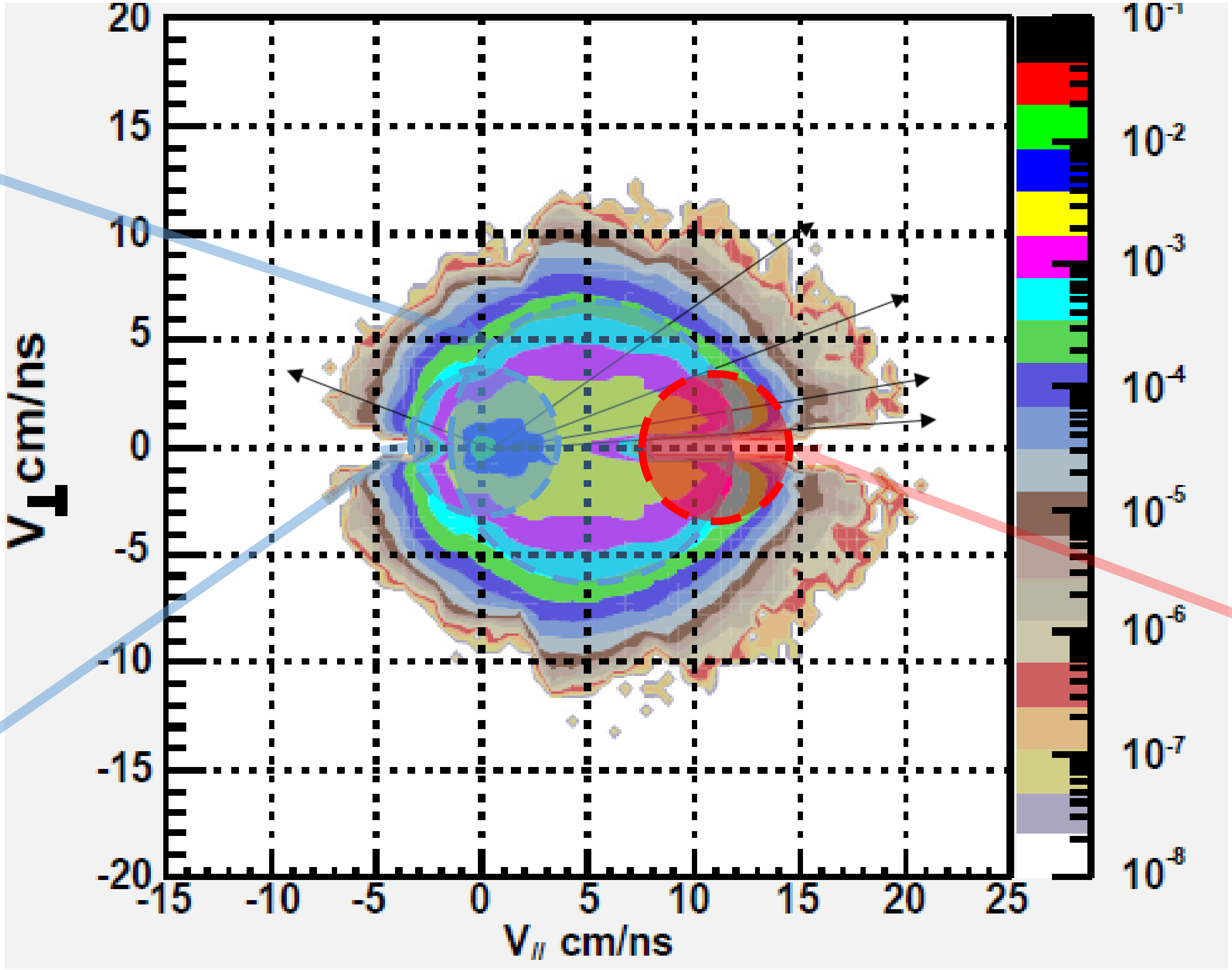

Quasi-projectile source

Quasi-projectile (QP) fragments

Employ the parameters of the three source fit to control the event-by-event assignment of individual charged particles to one of the three sources using Monte Carlo sampling

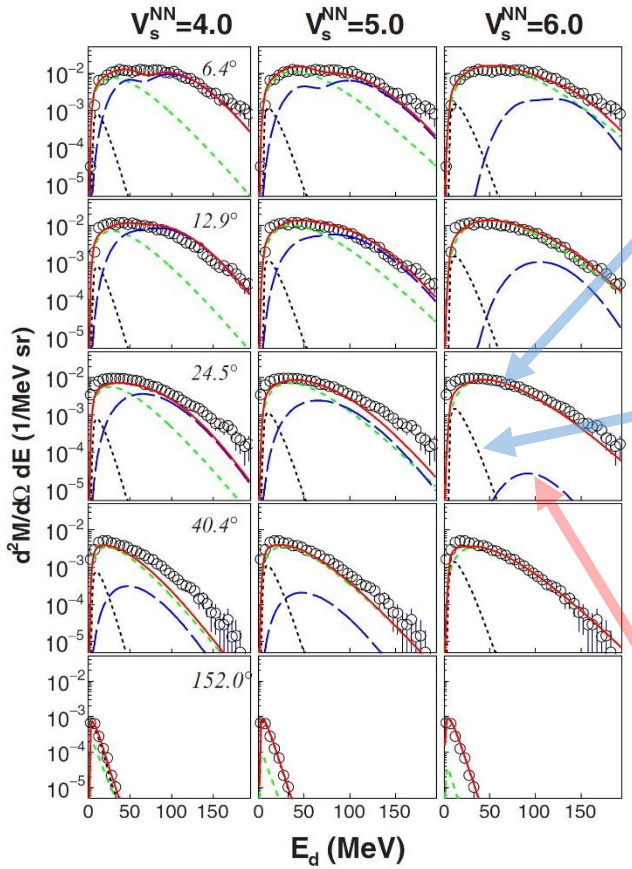

Nucleon-nucleon source

Quasi-target source

QP source $V_s^{QP} = 8.5 \pm 1.0 \mathrm{cm/ns}$

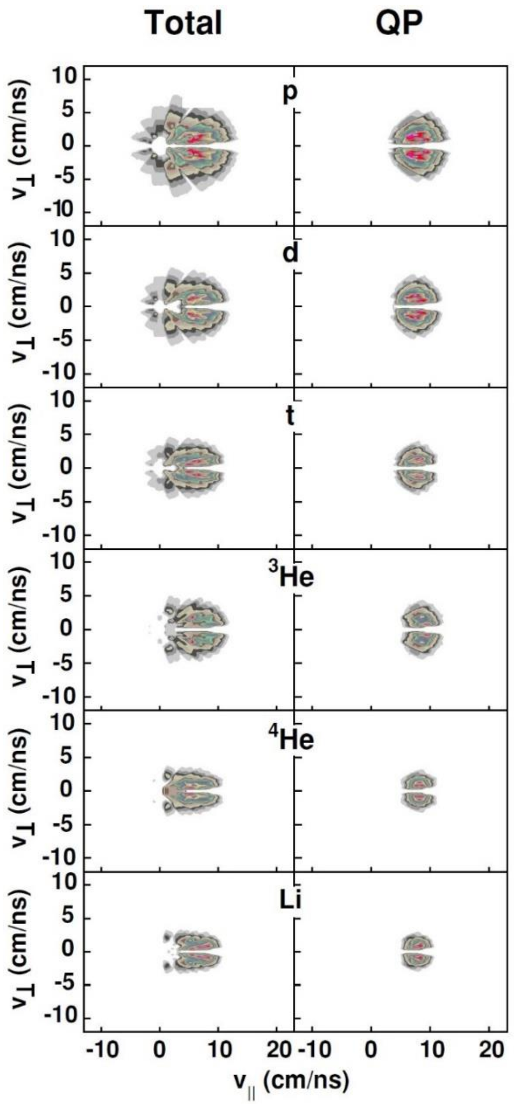

Y.-G. Ma, *et. al.*, PRC71, 054606, (2005) R. Wada, *et. al.*, PRC99, 024616, (2019)

Event-by-Event excitation energy

$$E_{\mathrm{ex}} = \sum_{i=1}^{M_{QP}} E_i^{kin}(CP) + \frac{3}{2} M_n T - Q$$

Mass excess

Kinetic energy of charged quasi-projectile particles

Temperature of protons from three source fit of proton

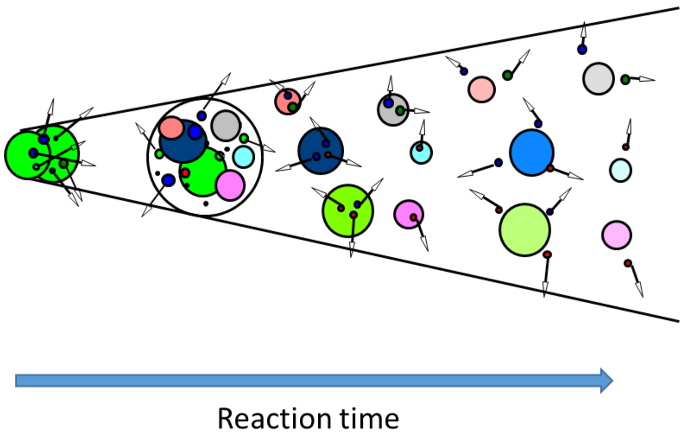

Neutron multiplicity in QP is approximated

$$M_n = A^{QP} - \sum_i^{M_{QP}} A_i(CP)$$

$$A^{QP} \approx Z^{QP}(1 + \frac{N}{Z})$$

N/Z ration of projectile

Apparent temperature

Fluctuation thermometer

S. Wuenschel, *et. al.*, NPA 843, 1, (2010)

Quadrupole momentum $Q_{xy} = p_x^2 - p_y^2$

$$T_{\text{fl}} = \sqrt{\frac{\langle Q_{xy}^2 \rangle - \langle Q_{xy} \rangle^2}{4m^2}}$$

Deuteron are used

T_{pol} and ΔT_{pol} are polynomial fit of T_{fl} and ΔT_{fl}, respectively

$$T_{\text{ap}} = T_{\text{pol}}(E*/A) + \Delta T_{\text{pol}}(E*/A) G(1)$$

Event-by-event

Gaussian random number

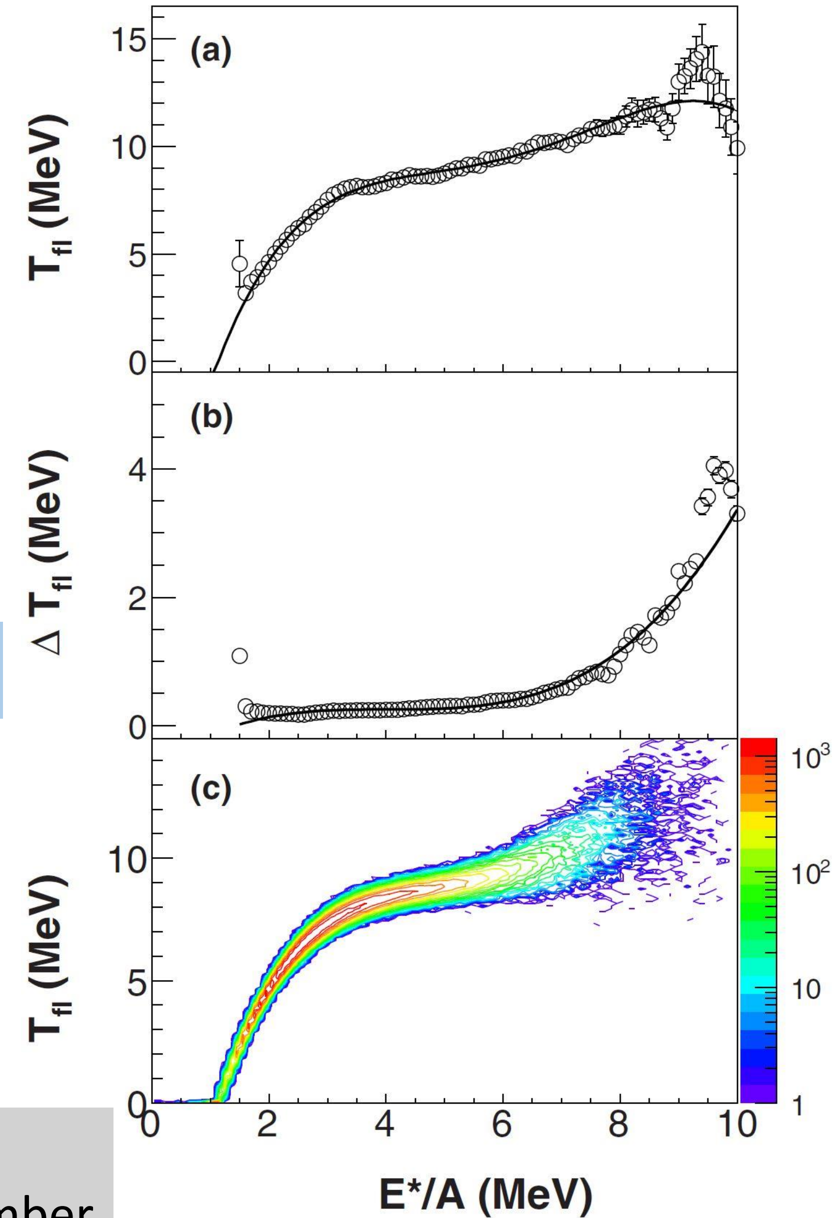

R. Wada, *et. al.*, PRC99, 024616, (2019)

Nuclear liquid-gas phase transition

The specific heat capacity of the collision process

$$\tilde{c} = \frac{d(E_{\rm ex}/A)}{dT_{\rm ap}}$$

Note its difference with c_v and c_p

Limiting temperature

$T_{\rm lim} = 9.0 \pm 0.4$ MeV

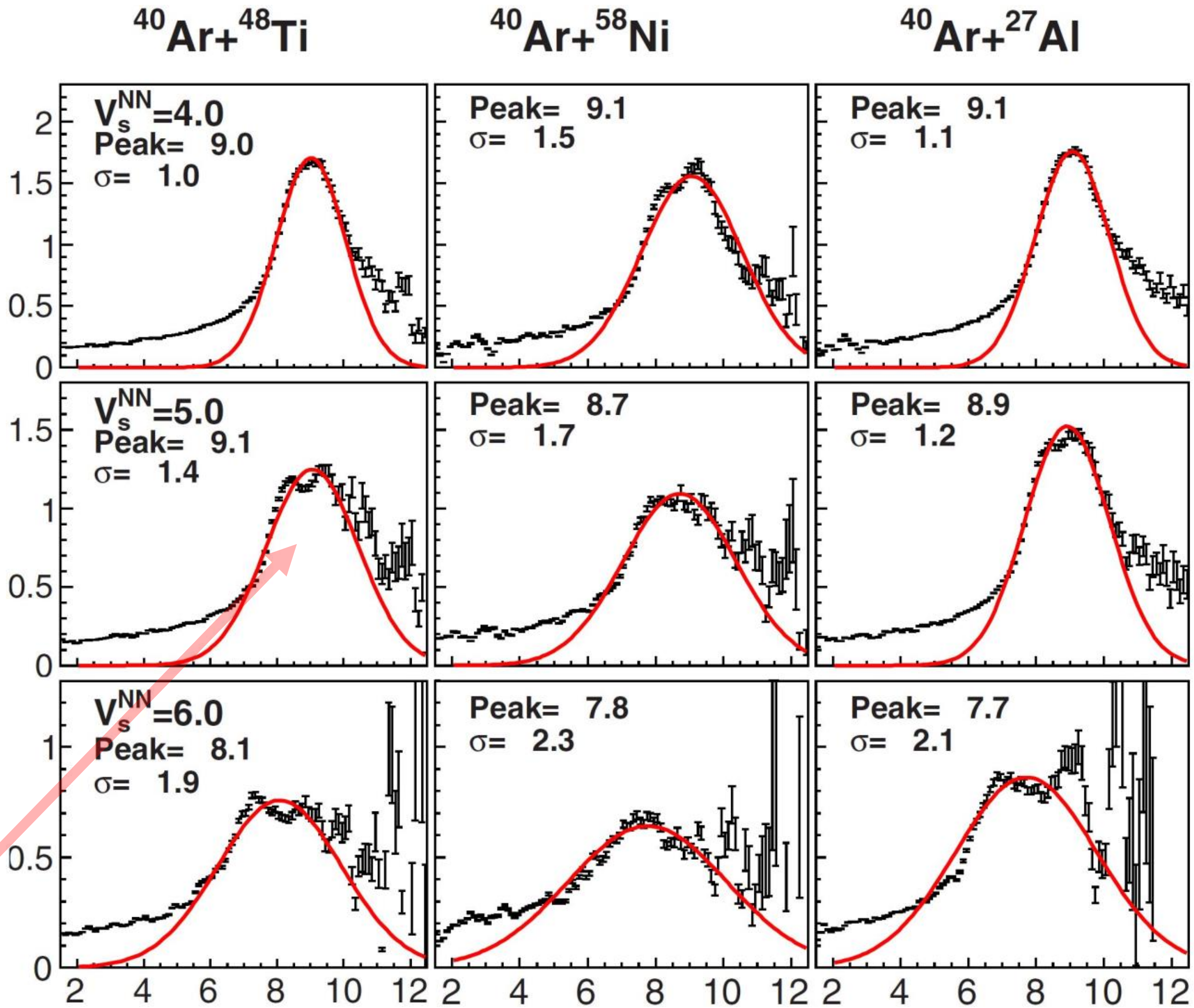

R. Wada, *et. al.*, PRC99, 024616, (2019)

Nuclear liquid-gas phase transition

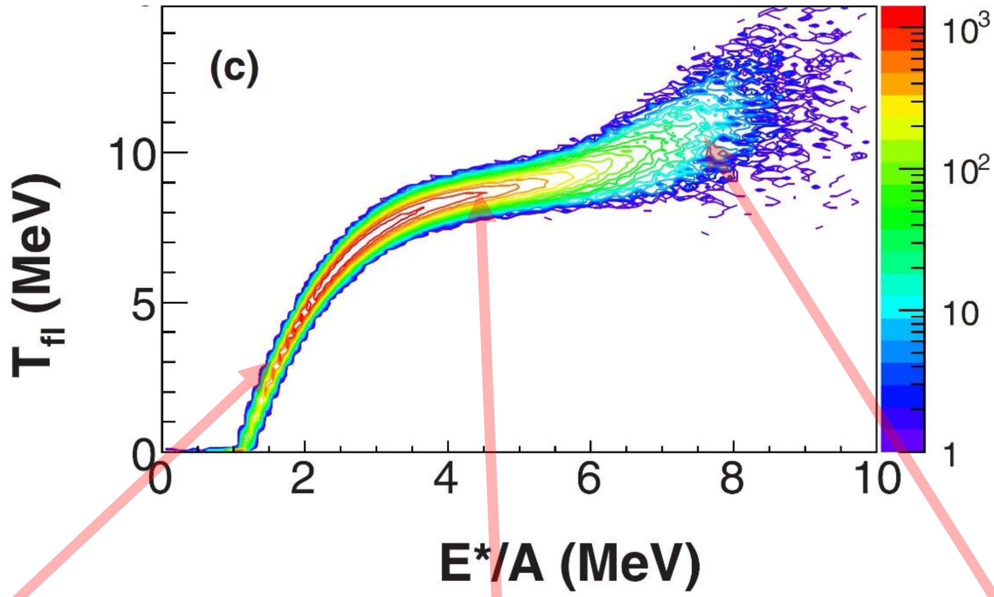

Charged particle multiplicity

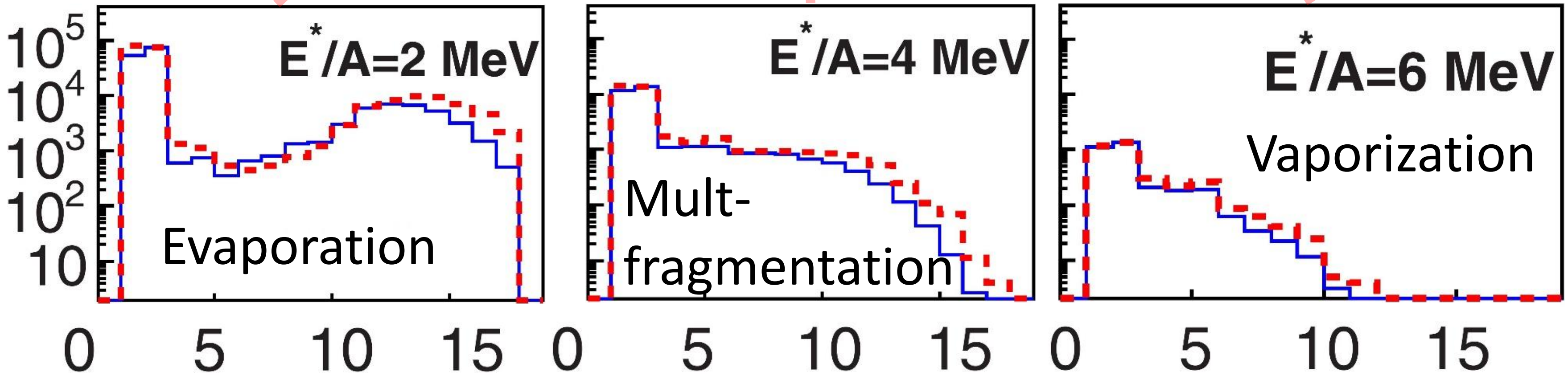

R. Wada, *et. al.*, PRC99, 024616, (2019)

Auto-encoder method

$Z^{QP} = 12$ events are used

Event-by-event charge-weighted charge multiplicity distribution $\mathrm{Z}M_c$

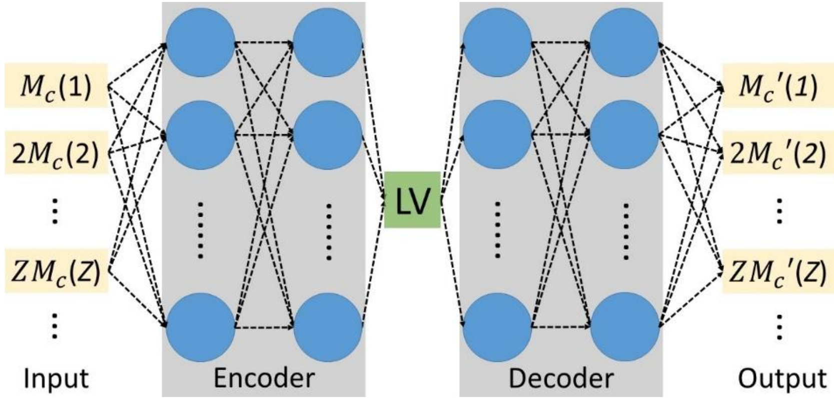

Reconstructed $\mathrm{Z}M_c$

The final state charge multiplicity of each QP event is encoded into the latent variable

Low excitation energy

intermediate excitation energy

high excitation energy

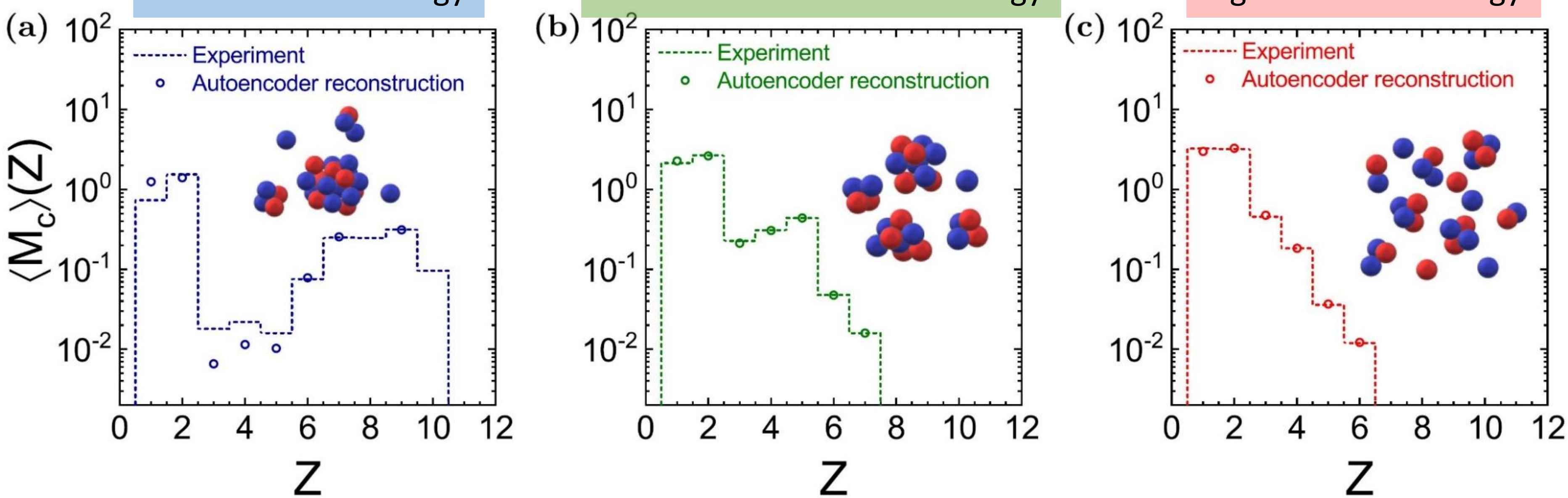

R. Wang, *et al.*, Physical Review Research **2**, 043202 (2020)

Auto-encoder method

The latent parameters of QP events are averaged in different apparent temperature T_{ap} or excitation energy E_{ex} bins

The auto-encoder network can identify different phases of quasi-projectile events directly from the charge multiplicity distribution, prior to any knowledge of T_{ap} or E_{ex}

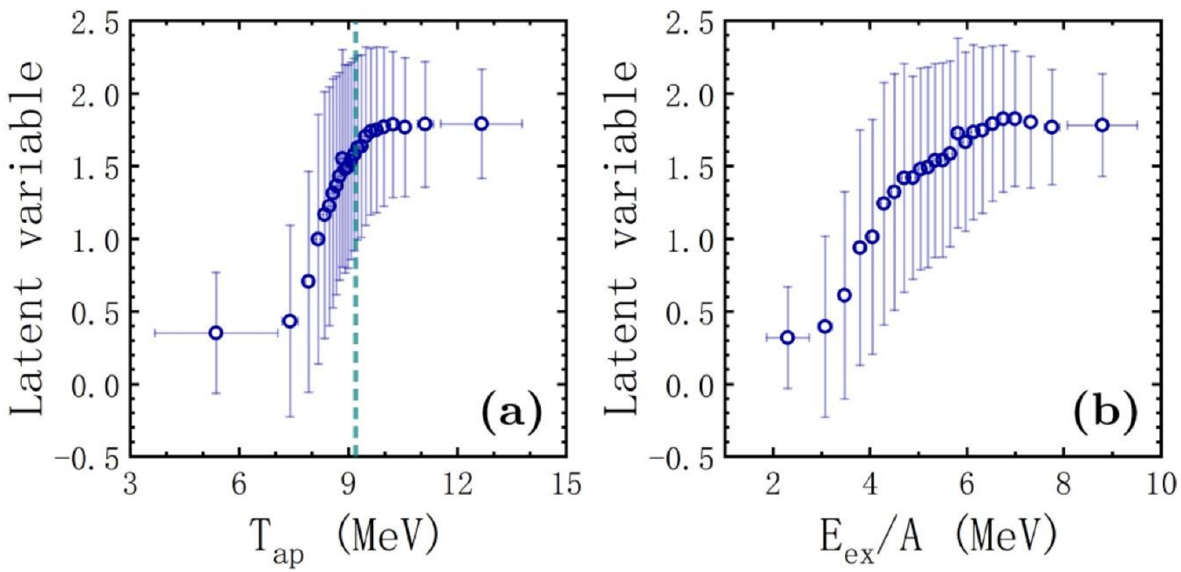

The sigmoid pattern indicates two different phases at low and high excitation energy or temperature

Each data point is averaged over 500 testing QP events

R. Wang, *et al.*, Physical Review Research **2**, 043202 (2020)

Limiting temperature from confusion scheme

Labeling QP events as liquid-like or gas-like according to a proposed transition temperature T'_{ap} or excitation energy E'_{ex}

Construct a neural network for supervised learning

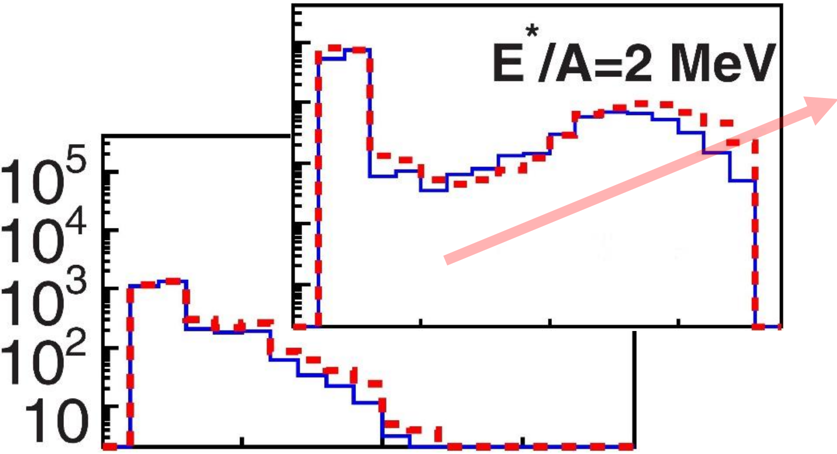

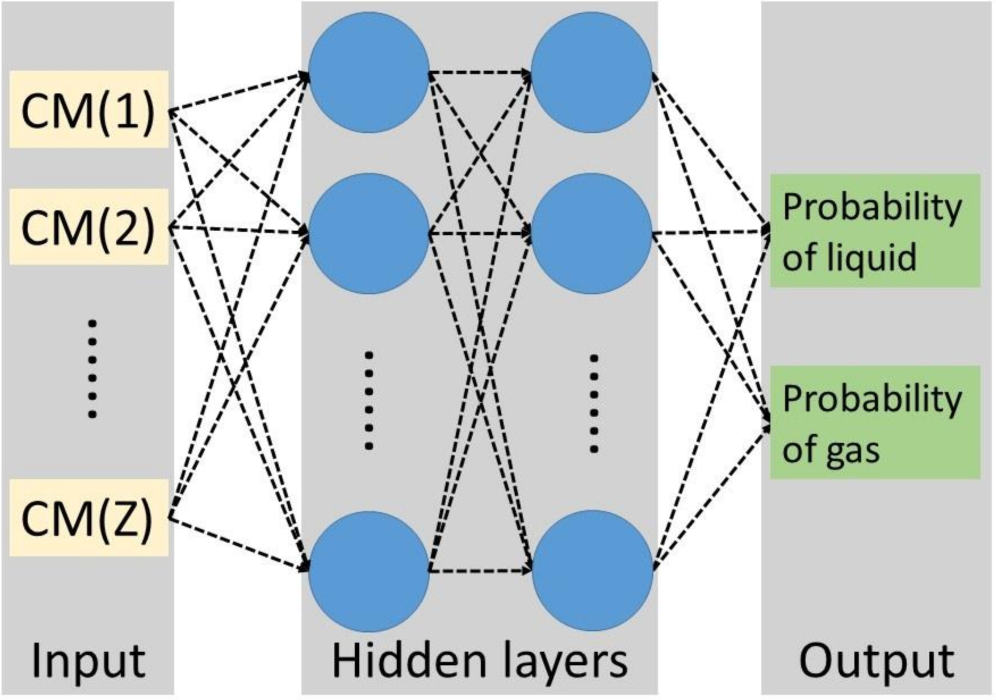

Limiting temperature from confusion scheme

Performance curve

(total testing accuracy as a function of T'_{ap} or E'_{ex})

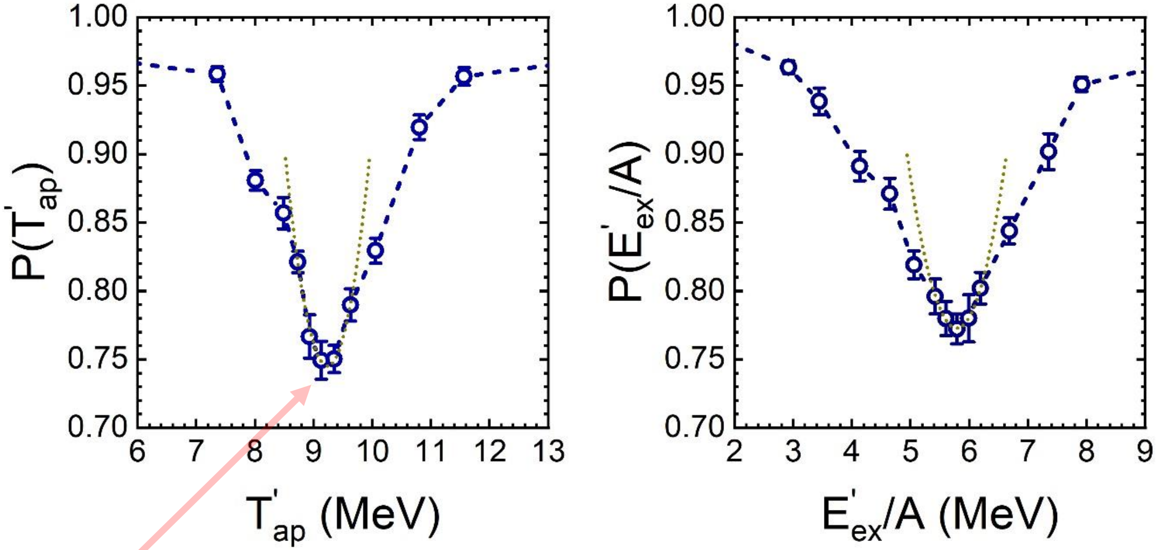

Limiting temperature from confusion scheme is about 9.2 MeV

Consistent with 9.0 ± 0.4 MeV from the traditional analysis of caloric curve

R. Wang, *et al.*, Physical Review Research **2**, 043202 (2020)

QCD phase diagram

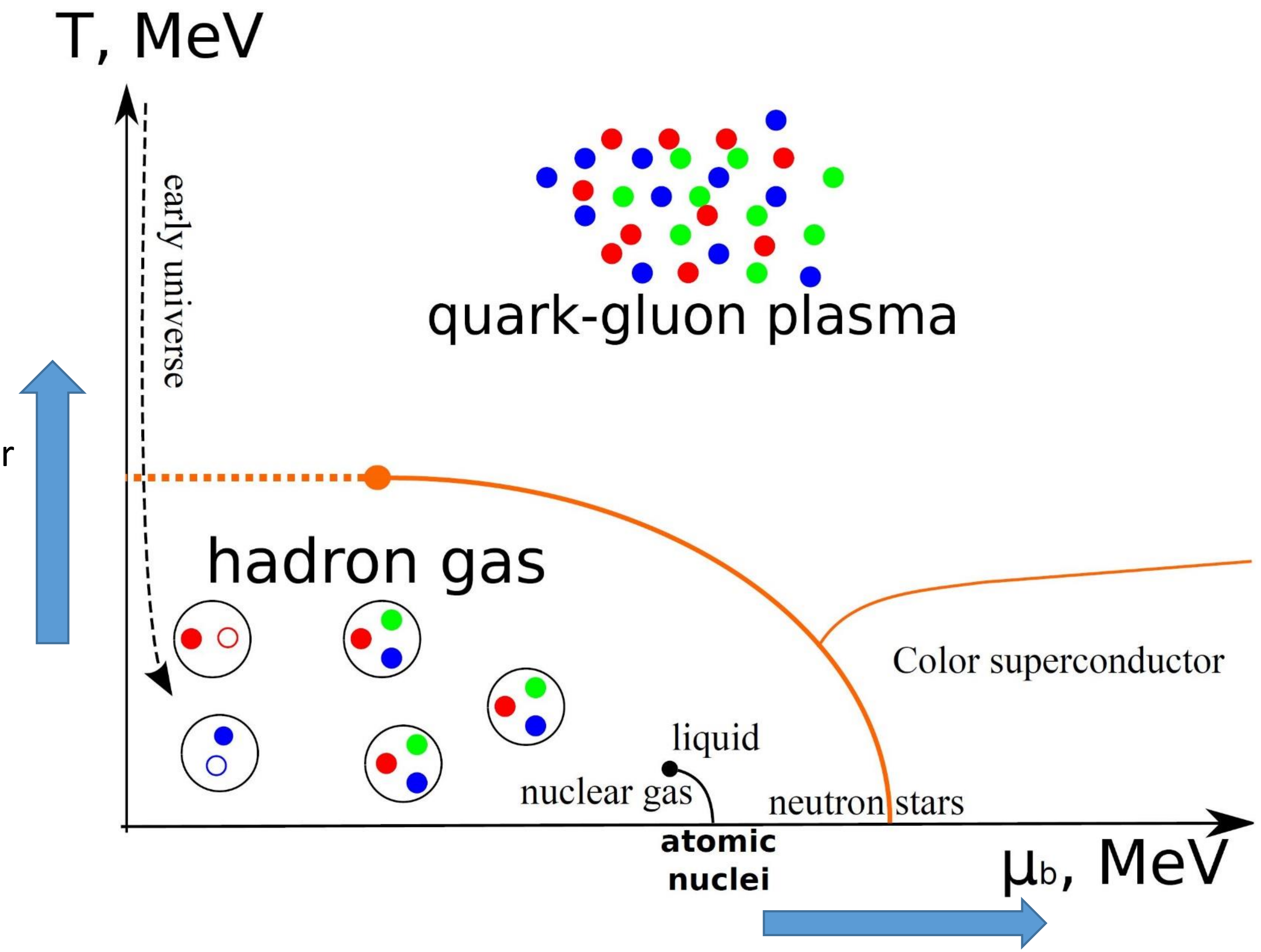

Second-order chiral restoration

First-order chiral restoration

Correlation length and fluctuation

Partition function

$$Z(h) = \mathrm{tr}\{\exp[-\beta H_0 + \beta h M]\}$$

Order parameter

$$\langle M(h)\rangle = \frac{1}{Z}\mathrm{tr}\{M\exp[-\beta H_0 + \beta h M]\}$$

Response of the order parameter

$$\begin{aligned} \chi &\equiv \frac{\partial\langle M(h)\rangle}{\partial h} \\ &= \beta\Big\{\frac{1}{Z}\mathrm{tr}[M^2\exp(-\beta H_0 + \beta h M)] - \frac{1}{Z^2}\mathrm{tr}[M\exp(-\beta H_0 + \beta h M)]^2\Big\} \\ &= \beta\big(\langle M^2\rangle - \langle M\rangle^2\big) \end{aligned}$$

Correlation length and fluctuation

$$M = \int d^3\vec{r} m(\vec{r})$$

$$\begin{aligned}\chi &= \beta \int d^3\vec{r} d^3\vec{r}' \left(\langle m(\vec{r}) m(\vec{r}')\rangle - \langle m(\vec{r})\rangle\langle m(\vec{r}')\rangle\right) \\ &= \beta V \int d^3\vec{r} \langle m(\vec{r}) m(\vec{0})\rangle_c\end{aligned}$$

Connected correlation function

$$\langle m(\vec{r}) m(\vec{r}')\rangle_c \equiv \Big\langle \left[m(\vec{r}) - \langle m(\vec{r})\rangle\right]\left[m(\vec{r}') - \langle m(\vec{r}')\rangle\right] \Big\rangle$$

Correlation length ξ

$$G_c(\vec{r}) \equiv \langle m(\vec{r}) m(\vec{0})\rangle_c \;\sim\; \exp(-r/\xi) \text{ at separations r} \gg \xi$$

Relativistic heavy-ion collisions

Since the QGP is expanding, the correlation length will not diverge, but freeze at a finite value

Also, it is difficult for the signal of the critical point to survive the hadronic stage

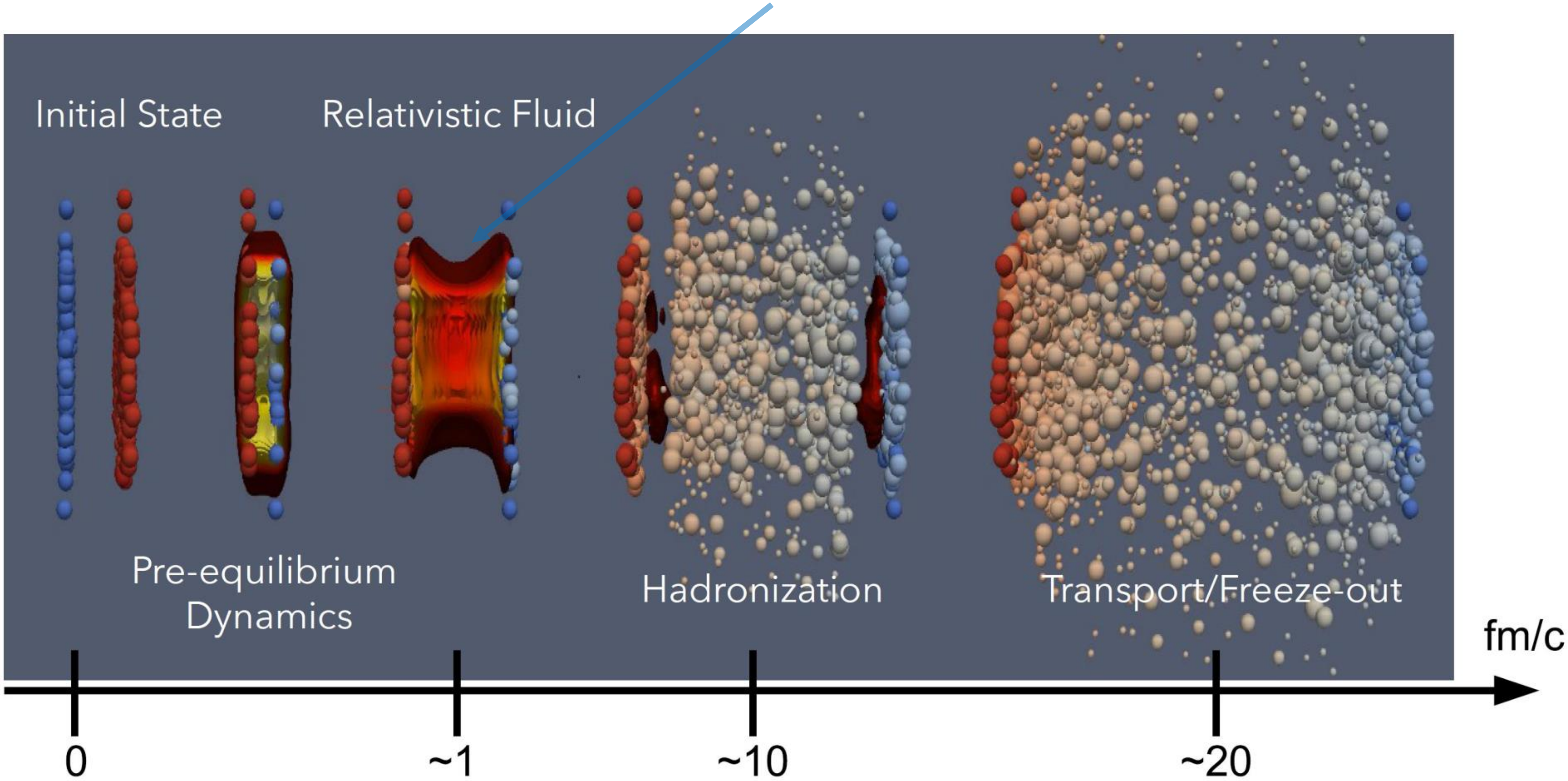

Net-proton number fluctuations

$$\delta N \equiv N - \langle N \rangle$$

$$\sigma \equiv \langle (\delta N)^2 \rangle \propto \xi^2, \;\; S \equiv \langle (\delta N)^3 \rangle / \sigma^3 \propto \xi^{4.5}, \;\; \kappa \equiv [\langle (\delta N)^4 \rangle / \sigma^4 - 3] \propto \xi^7$$

These moments without critical behavior follow from Skellam distribution (the difference between two Poisson distributions)

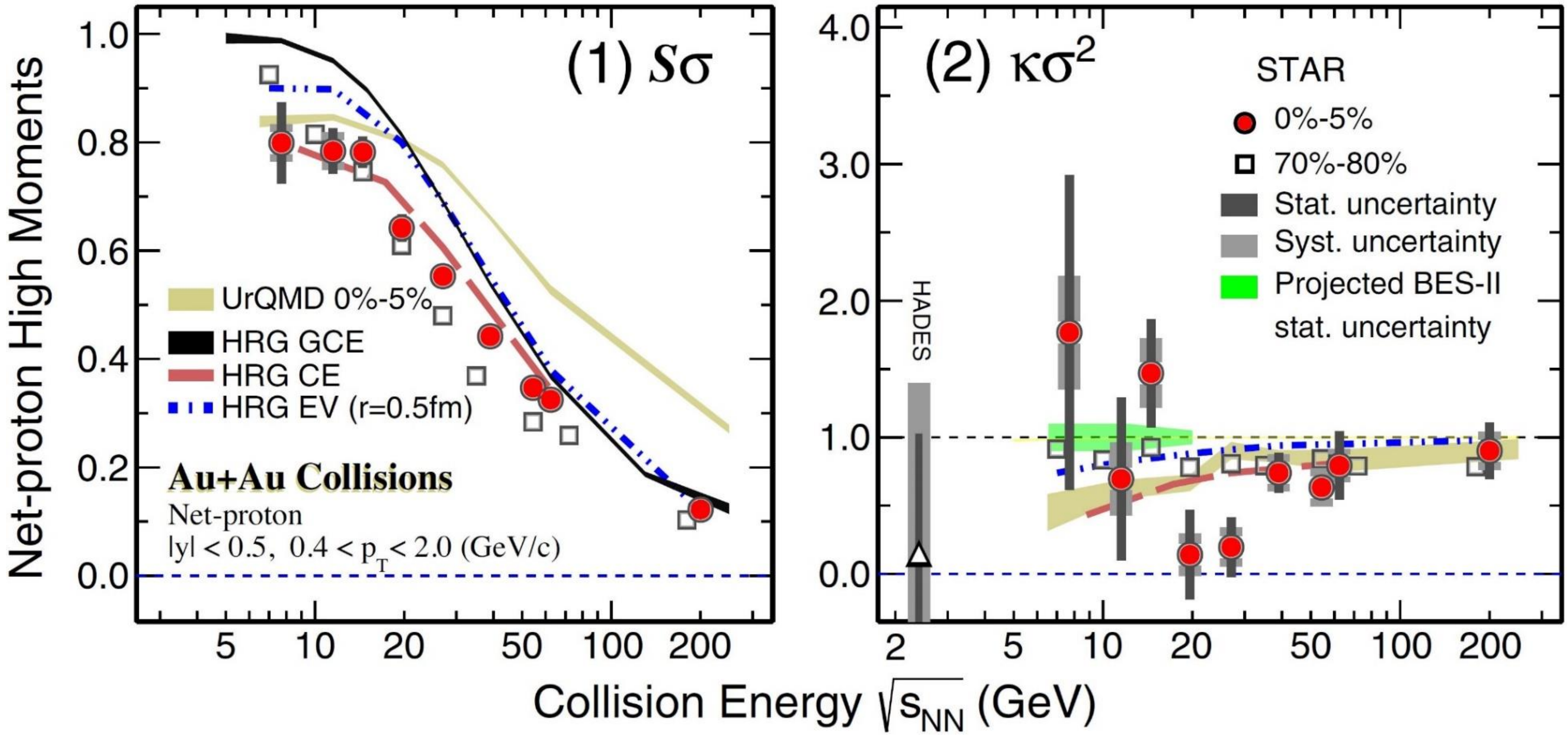

J. Adam, *et al.* (STAR Collabration), Physical Review Letters **126**, 092301 (2021)

QCD phase diagram with machine learning

Different EoS -> relativistic hydrodynamic model

Final state distribution $\rho(p_T, \phi)$ of charged pions

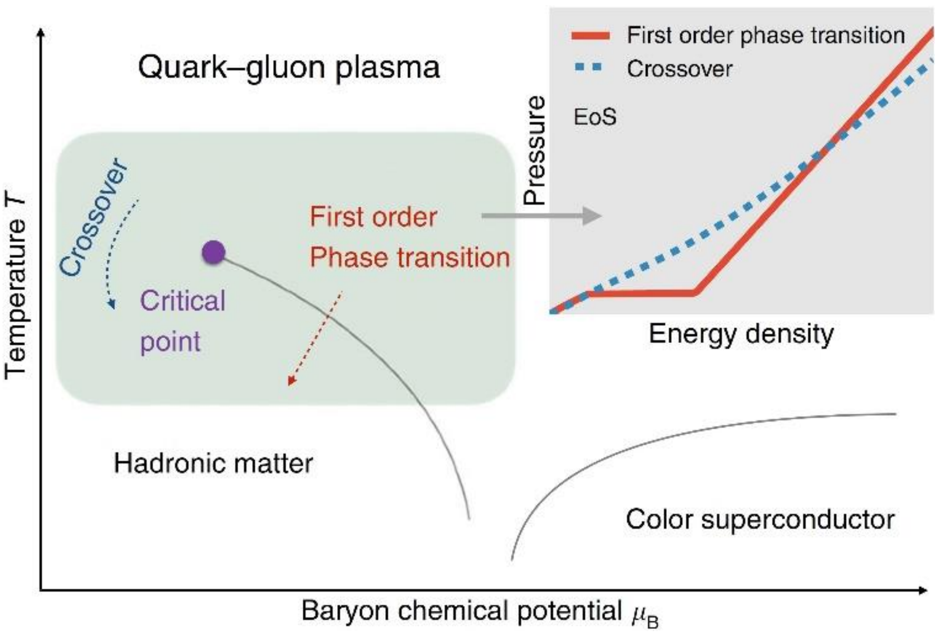

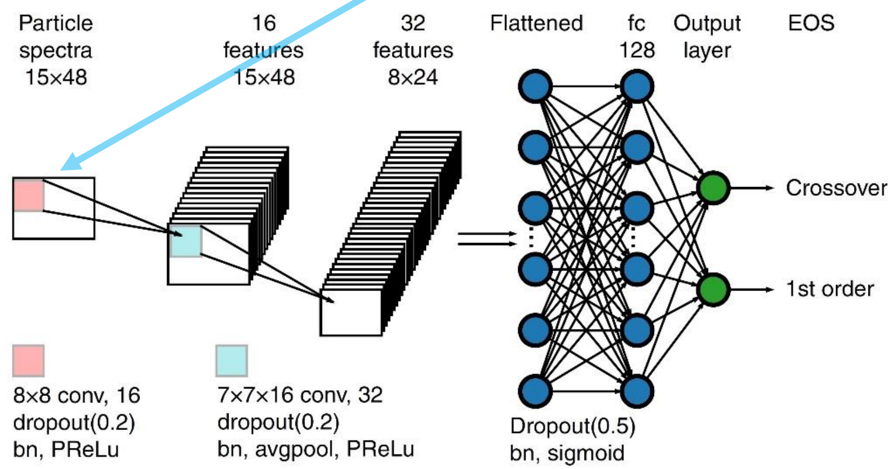

Testing data	Group 0	Group 1	Group 2
Number of events	4000	7343	10,953
Accuracy	$99.88 \pm 0.04\%$	$93.46 \pm 1.35\%$	$93.91 \pm 3.92\%$

L.-G. Pang, *et. al.*, Nature Communications **9**, 210 (2018)

Summary

Machine learning methods provide an alternative way of studying the complex nature of phase transition, yet more efforts are needed to obtain novel and informative results.

Main reference books

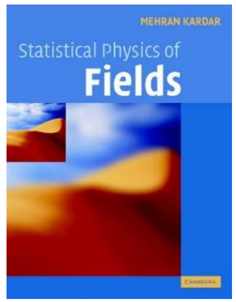

Further reading

S. S. Schoenholz et al., Nature Physics 12, 469–471 (2016)
K. Ch'ng et al., Physical Review X 7, 031038 (2017)
L. Li et al., Science Advances 4, eaap8672 (2018)
Y.–H. Liu & E. P. L. Van Nieuwenburg, Physical Review Letters 120, 176401 (2018)
M. Koch-Janusz & Z. Ringel, Nature Physics 14, 578–582 (2018)
J. Venderley et al., Physical Review Letters 120, 257204 (2018)
R. A. Vargas-Hernández et al., Physical Review Letters 121, 255702 (2018)
J. F. Rodriguez-Nieva & M. S. Scheurer, Nature Physics 15, 790–795 (2019)

Thank you

Convolutional neuron network

卷积神经网络

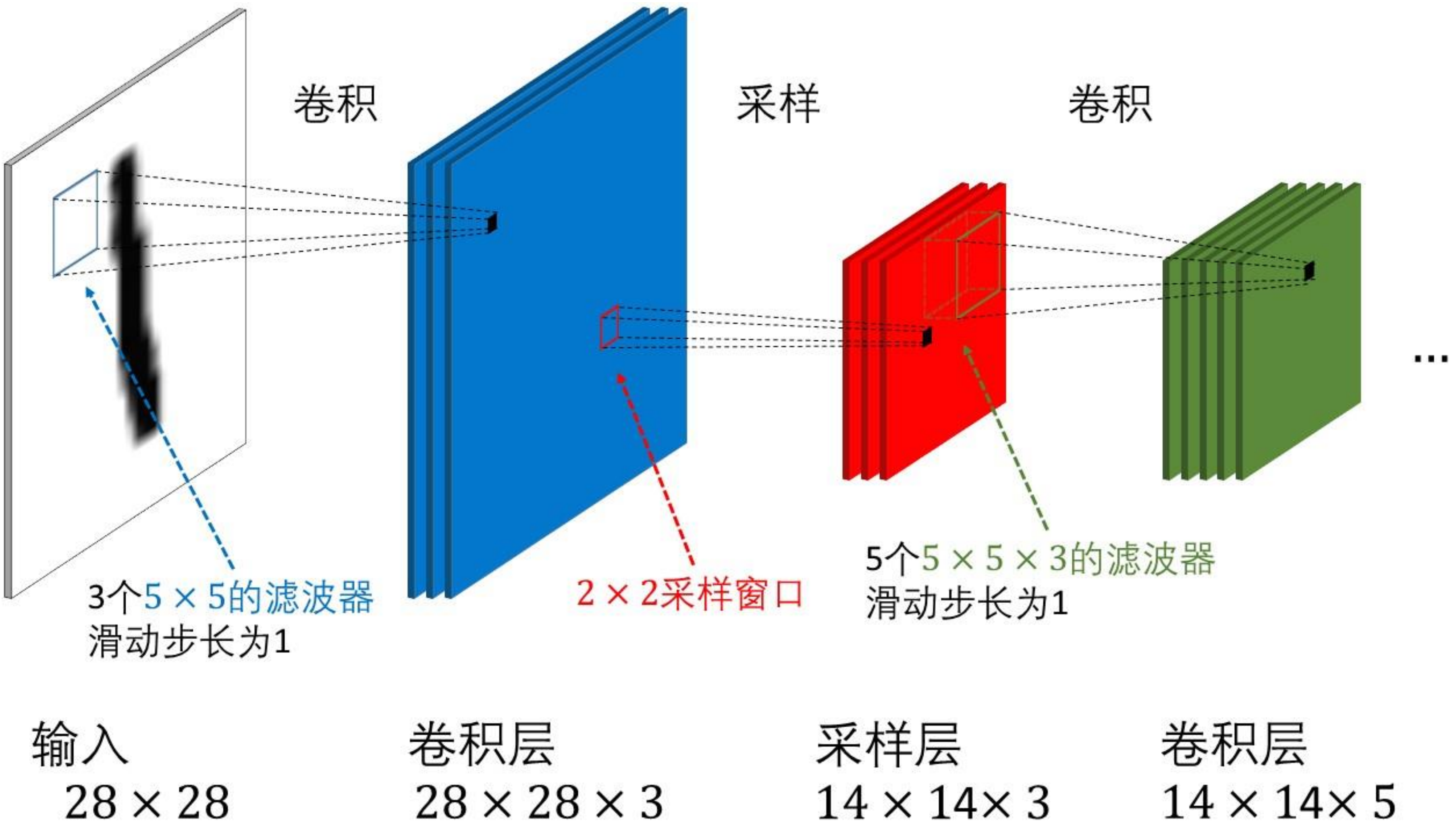

Convolutional neuron network

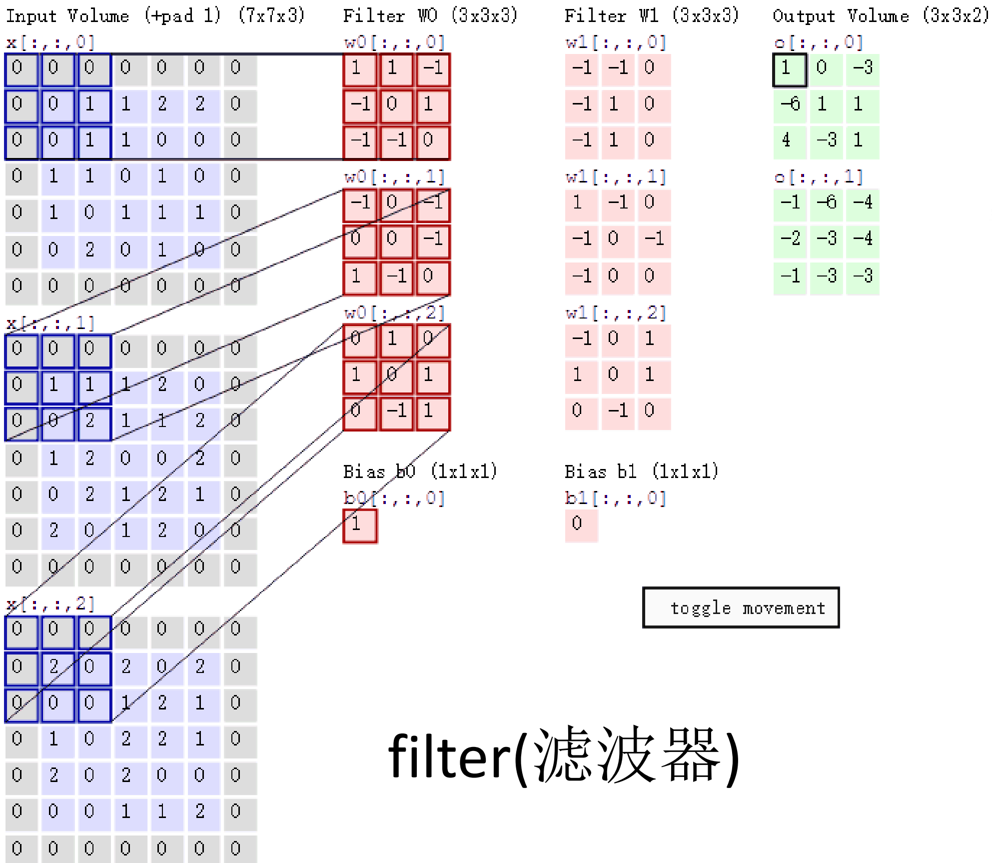

filter(滤波器)

pooling(池化/采样)

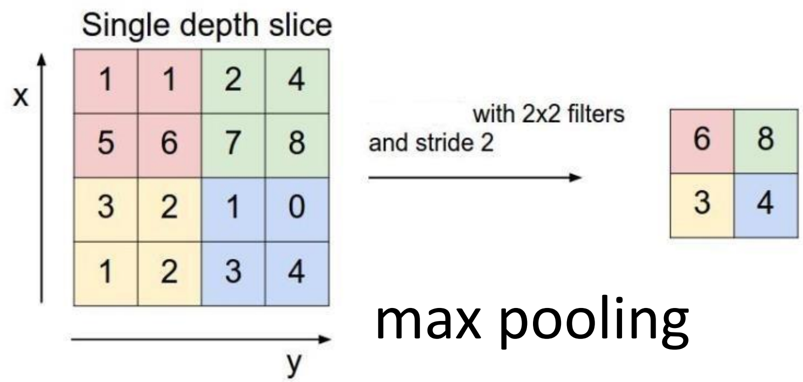

max pooling

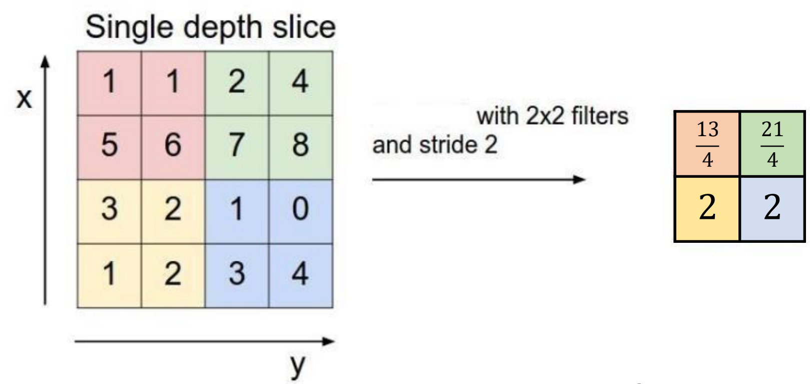

mean pooling

Goldstone modes

Order parameter $\psi(\mathbf{x}) = \overline{\psi} e^{i\theta(\mathbf{x})}$

$$\beta\mathcal{H} = \beta\mathcal{H}_0 + \frac{K\overline{\psi}^2}{2}\int d^d\mathbf{x}(\nabla\theta)^2$$

Decompose the variations in phase of the order parameter

$$\theta(\mathbf{x}) = \frac{1}{\sqrt{V}}\sum_{\mathbf{q}} e^{i\mathbf{q}\mathbf{x}}\theta(\mathbf{q})$$

$$\beta\mathcal{H} = \beta\mathcal{H}_0 + \frac{K\overline{\psi}^2}{2}\sum_{\mathbf{q}} q^2|\theta(\mathbf{q})|^2$$

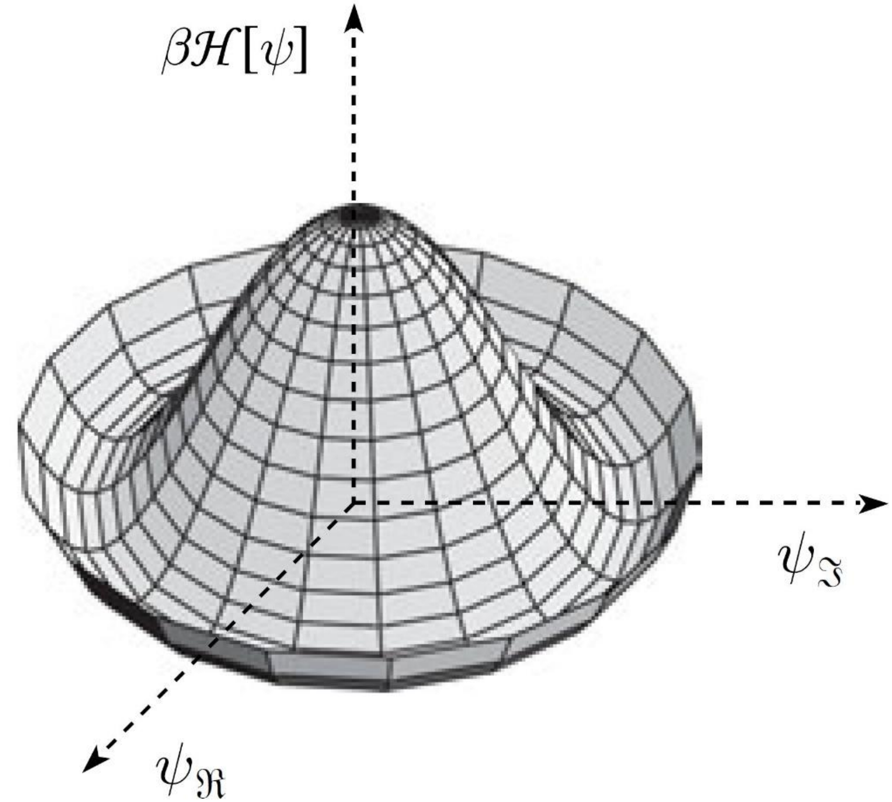

$$\overline{\psi}^2 \propto t$$

The energy of a Goldstone mode becomes very small a long wave length (q~0)